THE DEVELOPMENT AND IMPLEMENTATION OF AN IONIC

POLYMER METAL COMPOSITE PROPELLED VESSEL

GUIDED BY A GOAL-SEEKING ALGORITHM

A Thesis

by

JASON AARON VICKERS

Submitted to the Office of Graduate Studies of
Texas A&M University
in partial fulfillment of the requirements for the degree of

MASTER OF SCIENCE

May 2007

Major Subject: Mechanical Engineering

THE DEVELOPMENT AND IMPLEMENTATION OF AN IONIC

POLYMER METAL COMPOSITE PROPELLED VESSEL

GUIDED BY A GOAL-SEEKING ALGORITHM

A Thesis

by

JASON AARON VICKERS

Submitted to the Office of Graduate Studies of
Texas A&M University
in partial fulfillment of the requirements for the degree of

MASTER OF SCIENCE

Approved by:

Chair of Committee,	Won-jong Kim
Committee Members,	Alexander Parlos
	James Boyd
Head of Department,	Dennis O'Neal

May 2007

Major Subject: Mechanical Engineering

ABSTRACT

The Development and Implementation of an Ionic Polymer Metal Composite

Propelled Vessel Guided by a Goal-Seeking Algorithm. (May 2007)

Jason Aaron Vickers, B.S., Texas A&M University

Chair of Advisory Committee: Dr. Won-jong Kim

This thesis describes the use of an ultrasonic goal-seeking algorithm while using ionic polymer metal composite (IPMC), an electroactive polymer, as the actuator to drive a vessel towards a goal. The signal transmitting and receiving circuits as well as the goal seeking algorithm are described in detail.

Two test vessels were created; one was a larger vessel that contained all necessary components for autonomy. The second was a smaller vessel that contained only the sensors and IPMC strips, and all power and signals were transmitted via an umbilical cord. To increase the propulsive efforts of the second, smaller vessel, fins were added to the IPMC strips, increasing the surface area over 700%, determined to yield a 22-fold force increase.

After extensive testing, it was found that the three IPMC strips, used as oscillating fins, could not generate enough propulsion to move either vessel, with or without fins. With the addition of fins, the oscillating frequency was reduced from 0.86-Hz to 0.25-Hz. However, the goal-seeking algorithm was successful in guiding the vessel towards the target, an ultrasonic transmitter. When moved manually according to the instructions given by the algorithm, the vessel successfully reached the goal.

Using assumptions based on prior experiments regarding the speed of an IPMC propelled vessel, the trial in which the goal was to the left of the axis required 18.2% more time to arrive at the goal than the trial in which the goal was to the right. This significant difference is due to the goal-seeking algorithm's means to acquire the strongest signal.

After the research had concluded and the propulsors failed to yield desired results, many factors were considered to rationalize the observations. The operating frequency was reduced, and it was found that, by the impulse-momentum theorem, that the propulsive force was reduced proportionally. The literature surveyed addressed undulatory motion, which produces constant propulsive force, not oscillatory, which yields intermittent propulsive force. These reasons among others were produced to rationalize the results and prove the cause of negative results was inherent to the actuators themselves. All rational options have been considered to yield positive results.

DEDICATION

For all those I have depended on, and all those ever will depend on me

ACKNOWLEDGEMENTS

First and foremost, I would like to thank Dr. Won-jong Kim. He has been extremely helpful throughout my work on this research. Whenever any problems were encountered, he was always willing to offer a solution or the means to one. It was his courses in mechatronics that drove me towards this project, and will ultimately drive me towards my desired career. His suggestions and ideas were invaluable to this research and inspired me to my own.

I would also like to thank both Dr. Alexander Parlos and Dr. James Boyd for serving on my thesis committee. It was a privilege to work with them. Special thanks are due to Mr. James Sajewski who aided in the creation of the first test vessel by producing it on the rapid prototyping machine in the Texas A&M materials lab. My thanks are owed to Dr. Kwansoo Yun who helped me initially test the IPMC material and helped me around the lab. I also thank Dr. Donald Leo and Dr. Barbar Akle at Virginia Polytechnic Institute's Center for Intelligent Material Systems and Structures for supplying the IPMC material that was used in the experiment.

Thanks to all my friends and classmates throughout my career as a mechanical engineer at Texas A&M. They have been a priceless part of my education, and it has been an honor to work with them. I wish all of them the best as they begin their careers.

My parents, Herb and Sherrie Vickers, have played a critical role in my education and have helped me along every step of the way, however they could. They have always been behind me, pushing me to succeed. It is my hope that with my education and abilities, I will be able to pass this vast generosity and love along.

To my family and friends not mentioned, each and every one has helped me become who I am today and has driven me to succeed in one way or another. For this, I am grateful.

TABLE OF CONTENTS

LIST OF TABLES

LIST OF FIGURES

1   INTRODUCTION

1.1 History

Much has been accomplished through innovations in the field of material science. Most of human history is chronicled by the advances in technology made available through advances in material science. The Stone Age marked the use of crude tools, created from stone or even human bone. The Bronze Age introduced bronze, copper and tin to tools and ornaments. The malleability of this metal allowed the creation of more intricately shaped tools. The advent of the Iron Age allowed further advances to be made.

New materials and new uses for materials are discovered continuously. Much effort is and has been placed in the research and development of smart materials. These materials are called "smart" because they respond to an external stimulus other than stress or strain. Smart materials can react to external stimuli such as an applied voltage or magnetic field. Some respond to temperature, pH level, or even gas absorption.

With such a diverse group of materials, the possibilities are limitless. Certain "smart structures" utilize smart materials to relay structural information such as damage or load. Shape memory alloys such as Nitinol (TiNi) undergo a martensitic phase transformation when a thermal gradient is applied, returning to its original condition when the thermal gradient is removed. Piezoelectric materials respond to applied electric fields with a mechanical change and vice versa.

This thesis follows the style of *IEEE Transactions on Automatic Control*.

The history of robotics can be traced all the way back to the clepsydra, a clock which used water, a float and a series of gear to keep track of time. This device originated as early as the 14th century B.C. [1]. In the 1890's Nikola Tesla experimented with remote control vehicles and many of his inventions paved the way for modern robotics [2]. In 1956, Devol and Engelberger decided to create fact from Isaac Asimov's fiction and form the company Unimation which went on to create the Unimate, used to spot-weld and remove castings at General Motors [3]. Though this robot was pre-programmed to do one certain task over and over, it gathered interest in the field and eventually smart robots that could perform autonomously were created.

Using memory and logic, a machine called "Shakey," created in the late 1960's independently navigated its indoor environment [4]. Not content with only working inside, a group at Stanford attempted to navigate an outdoor environment in the 1970's. Even today, the Defense Advanced Research Projects Agency (DARPA) holds the DARPA Grand Challenge, a contest in which many groups compete with their robots to navigate a desert course through GPS waypoints. Not until 2005 did a team complete the task, traversing a 132-mile course through the desert, where the fastest time was just under 7 hours and only 5 of 25 teams actually finished [5]. The 2007 challenge is to navigate a 60-mile course in an urban environment in less than 6 hours. There is still much work to be done towards creating a fully autonomous vehicle that can be left unsupervised, but the implications of such a feat are astounding.

1.2 Electroactive Polymers

Electroactive polymers (EAPs) respond to electric stimulation with a considerable shape change [6]. These materials have only been discovered in the past decade and are very promising for many reasons. In biomechanics, the field of study involving the synthesis of parts similar to those found in living organisms, EAPs are being considered for use as actuators similar to muscles. EAPs exhibit high strains and relatively fast actuation times when compared to shape memory alloys. Two categories of EAPs exist, based on their mode of activation. Electronic EAPs respond to electric fields, have a relatively high actuation force, and are able to maintain constant strains under constant voltage, yet require high voltages to actuate. Ionic EAPs, however, require very little energy to actuate, though generally do not hold constant strains under applied DC voltages. The working principle behind ionic EAPs is the diffusion of ions through the material. The Ionic Metal Polymer Composite material (IPMC) belongs to the ionic EAP class.

1.3 Structure and Working Principle of IPMC

The IPMC material belongs to the ionic EAP class where actuation is caused by ion diffusion. It is created using a roughed up sheet of base polymer, such as porous fluorinated polymers like DuPont's Teflon$^®$ or Nafion$^®$ [7]. The polymer is roughed up using sandblasting and washing methods, then plated using electro-chemical reduction. The polymer is plated with a noble metal such as platinum or gold.

The actuating action of the IPMC material is due to ion migration from the anode to the cathode due to the electrostatic forces induced by the applied voltage. The porous polymer substrate allows for ion migration between polymeric chains. Figure 1.1 shows a schematic representation of the IPMC structure.

Noble Metal
(Au or Pt)

Ion

Base Polymer

Dispersed
Water
Molecule
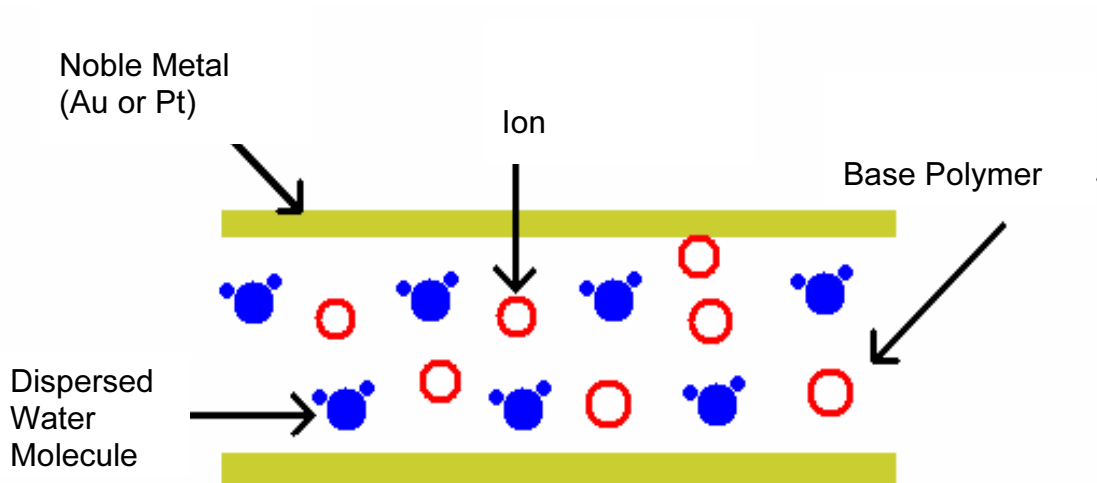
Fig. 1.1: Structure of IPMC material

As an electric potential is applied across the electrodes, the cations (typically Na^+ or Li^+) migrate from a neutral position to the anode. As they migrate across the polymer, water molecules are caught by the ions and swelling occurs on that side, bending the IPMC material as in Figure 1.2. This expansion and contraction is what causes the bending in the material. Relaxation occurs in the material as voltage is held constant and the IPMC material returns to its original position. This is due to the movement of the water molecules back through the material.
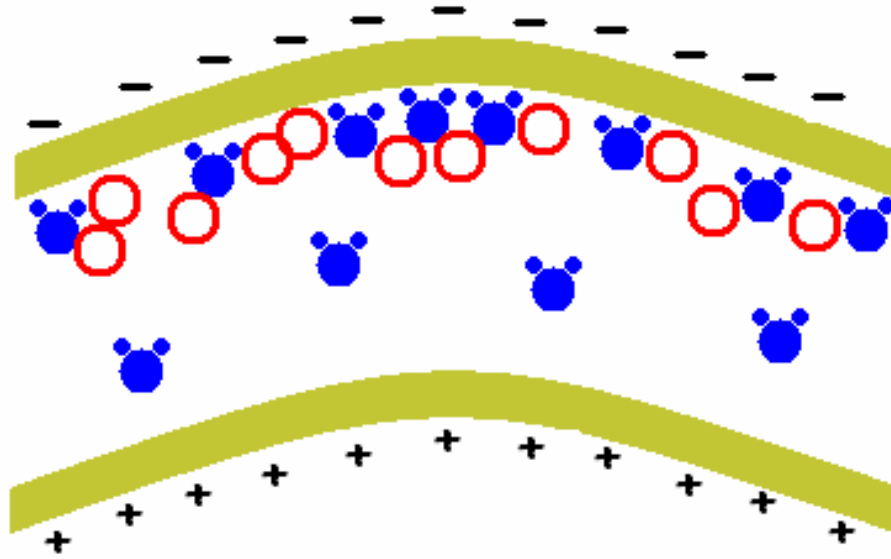
Fig. 1.2: Actuated IPMC material showing cation attraction to anode

1.4 Applications of IPMCs

The IPMC material is very attractive because of its high efficiency and high strains, and many uses of the material have been considered in a variety of fields. The fields of biomechanics, robotics, and medicine are just some of many fields studying and implementing the use of IPMC material.

1.4.1   IPMC Use in Medicine

Because it has such low power consumption and is highly efficient, many medical applications are being researched and developed for IPMCs. A cardiac-assist muscle has been developed and tested [8]. It uses the IPMC actuation to squeeze the heart itself, much like the compressions performed during Cardiopulmonary Resuscitation (CPR). This is promising because the actuator is only around the heart,

not contacting the blood flow in the heart which could result in clotting or thrombosis. A similar use involves a band around the eye to correct vision, shaping a myopic or hyperopic eyeball to focus images correctly on the receptors.

Pumps have been created for the purposes of *in situ* applications. Peristaltic pumps, or tube-shaped pumps that transport matter, similar to an intestine are created using proper placement of electrodes about the tube.

Smooth muscle actuators work in much the same way as the peristaltic pumps do. Progressive actuations in the muscle to create a traveling wave allow these actuators to work like veins, arteries, or other transporting body parts. Using IPMC as an exoskeleton to enhance the human body or as a prosthetic device has been researched as well [8]. Because the material can be used both to sense and actuate, sensors are not required and closed-loop control can be implemented without using other sensors.

It is the hope of many researchers that IPMCs can one day be used inside the body. The material shows promise in medicine because it can be used in a variety of ways and requires little power input for significant strains.

1.4.2   IPMC Use in Robotics

One major application of IPMC material is in the field of sensors and actuators. As a strain gauge, the material performs well under both static and dynamic perturbations. Though the output voltage is relatively low, it is sufficient to detect even small deflections.

Actuator applications such as grippers are being researched to develop control algorithms that apply constant force and displacement even as the material becomes dehydrated, permitting use in atmospheric environments [9].

Unusual applications are being considered for the material as well. Using the material as wipers on a solar panel on a solar-powered vehicle in space has been explored [7]. Because of the high efficiency of the material and its bending actuation, it is the ideal material to select in such an application. Any debris that was to hinder the energy collection potential of the solar cells would be removed, allowing the device to work at its full potential.

1.4.3   IPMC Use in Biomimetics

Much work has been put forth into discovering uses for IPMC materials as muscles and fingers [10], largely due to their low power consumption and high strains. Using only 25 mW with a 5-V power supply, the Artificial Muscle Research Center in New Mexico was able to lift over 10-g using four 0.1-g IPMC strips. This motion could be used to collect samples in space or even eventually replicate the motion of a human hand either *in vivo* or in an automaton.

Research has been done to mimic the motion of a bird's wing [11]. The research measured lift and thrust forces on a specially cut IPMC strip to mimic the motion of a real bird wing. Though large displacements were observed, the research concluded there was insufficient lift and thrust for flight.

Because IPMC materials rely on the presence of water molecules to perform, many aquatic applications have been looked at. When the IPMC material is fully

immersed in water, evaporation of water molecules from the polymer is not an issue. A group in Estonia replicated the mechanics of a ray's swim stroke [12]. Using only six grams of IPMC material on a 60-g robot, the group attained a maximum speed of 5 mm/s, an impressive feat when the fact that over half of a fish's body weight is muscle.

A Korean group used the IPMC material with a pulse-width-modulation (PWM) algorithm to create an undulatory fin on a robot tadpole that works with a PWM code to supply the power [13]. This undulatory motion is best described by a wriggling action or a wave motion. The motion of the tadpole is dictated by the frequency of undulation or oscillation and the potential between the electrodes. At a 4-Hz frequency using an IPMC fin with a mass of 50 mg, the 16.2-g tadpole was able to achieve a velocity of 23.6 mm $\times$ s^{-1}.

A fairly simple robot to test the propulsive power of an IPMC fin was used by a group from the University of Nevada's Active Materials and Processing Laboratory [14]. This robot was similar in shape to the undulatory tadpole aforementioned, but did not perform the wriggling action, only oscillatory actuation. Placed inside a column of water, the IPMC strip affixed to the tadpole-shaped test rig was connected to a load cell, and it was calibrated with the fin and test rig in place to negate the effects of gravity. The IPMC fin was a trapezoid with overall length of 25 mm and greatest width of 15 mm. With a 5-V driving voltage to the IPMC fin, a 0.004 N force was generated. To propel a vessel through the water, this propulsive force must overcome the drag force in the water.

A Japanese group working with a number of research centers developed a biomimetic snake that swam through water [15]. This snake consisted of three segments, each connected by a 2 × 20 mm strip of IPMC material. The body was made from styrene foam so the apparatus was extremely lightweight. The voltage source was a 5-V peak-to-peak amplitude square wave with a period of 1.6 s. The maximum speed generated was 8 mm/s at this period of oscillation. Various media were used to dope the snake robot; among them were sodium (Na^+), cesium (Cs^+) and tetraethylammonium (TEA^+). The doping method that resulted in the greatest robot speed was Na^+, though it consumed the most power. The slowest robot speed occurred when the IPMC was doped in TEA^+, but it consumed the least power. The robot doped in Cs^+ gave average characteristics.

Eamex Corporation in Japan has used IPMCs to produce an artificial fish that can move sporadically about a tank without any input or maintenance for some time [16]. The fish are not controlled by any means; they are only designed to be buoyant enough to replicate the motion of an aquarium fish. It is the focus of this project to develop a "goal-seeking" control to work with the IPMC material when used as a fin.

1.5 Goal-Seeking Applications

A number of control algorithms are used in robotics. Most projects use either goal-seeking, wall-following, obstacle-avoidance, or a combination of those three. For the purpose of this thesis, navigating in the open water, goal-seeking is the only logical choice. Much work has been carried out to implement goal-seeking algorithms in

various applications. Although much of the previous work has been with land-based robots using wheels for propulsion, the same basic control principles apply.

Research has been done on line of sight navigation towards a moving goal [17]. To accomplish this, the kinematics of the robot and the goal were modeled and the kinematic relationships were derived from the model. The velocity data was collected from an observer position which relayed it to the robot to determine the next velocity vector for the robot. To keep the robot on track between measurements, a Kalman Filter was implemented for state estimation. This vehicle was able to reach the goal, independent of the goal's path, and could even navigate obstacles with the addition of an obstacle avoidance algorithm. One problem that this line-of-sight navigation method faces is what would happen when the robot or goal goes out of the line of sight.

A project simulating a number of control algorithms used wall-following, obstacle-avoidance, and goal-seeking logic independently and the combinations of two or more of them [18]. The goal-seeking simulation used a local coordinate system and velocity vector of the robot with the relative orientation of the goal from the robot. Though this was only a simulation of the robot, it is important to note that, as predicted, just plain goal-seeking is not sufficient in an obstacle-laden environment. Goal-seeking by itself should only be used in an open environment, as is the case for the IPMC boat.

Many other goal-seeking or tracking algorithms use fuzzy logic to determine the robot action. One such project created an autonomous vehicle that used a number of ultrasonic, piezoelectric, and infrared sensors to direct it around walls and obstacles, along a path, and towards an infrared goal as an ultimate objective [19]. The fuzzy logic

implemented could be divided between each of the algorithms independently. Right and left wall following, goal seeking, and obstacle avoidance gave a total of 52 fuzzy logic rules. In addition to the fuzzy logic rules, a hierarchy was given to prioritize the actions. The results showed that the robot could follow paths, walls, and travel towards a goal. It could even follow sparse edges outdoors such as the edge crops. This research showed that there can be a lot of versatility in robotics, between power supply (diesel or electric); and control algorithm (wall-following, obstacle-avoidance, or goal-seeking).

One intriguing project was the "Army Ant," designed and built by a team at Virginia Tech was built to move cargo from place to place [20]. Two components were used for goal-seeking: infrared for direction and ultrasonic for distance. The group made a number of identical robots to work together as a group to achieve a common goal. Their objective is to pick up a crate and move it towards a target. When the robots are all lifting the crate, the control algorithm to move the crate to the target begins. This target is selected by means of an infrared beacon placed at a goal. Using the infrared sensor, one robot orients itself towards the goal, and the other robots detect changes in the force vector and orient themselves to maintain the original force vector and move at a constant velocity towards the target.

Using ultrasonic signals to detect distances on all sides from the device, the GuideCane allows visually impaired users to know what is located all around them [21]. The GuideCane uses a number of ultrasonic rangefinders, a pair of transmitters and receivers, to determine the distance from certain objects. If a foreign object comes within close proximity, the GuideCane steers itself using a motor at the end of the cane

to steer the cane away from the object. The user feels this motion and follows. This research proves that ultrasonic signals are repeatable and reliable and useful in range finding and control algorithms.

1.6 Contributions of Thesis

The driving contribution of the thesis is to further develop a novel use of the IPMC material. Though the material has been used as a undulatory fin in prior research, it has yet to be used as an oscillating fin in a "goal-seeking" application. The utility of such an application is broad. With such a high efficiency material, only a small power supply is needed. The motion is quiet as it moves in a gradual manner, and it replicates the motion of a fish fin, making it an ideal choice for an undetectable aquatic vessel.

The research performed is aimed at showing the usefulness of the material in a global-scale control setting, where the whole vehicle is controlled, rather than just a single actuator. Various "goals" can be used in the "goal-seeking" algorithm. A Global Positioning System (GPS) input, for example, would easily allow a user to enter a set of coordinates and based on the current location and direction, the vehicle would go to the desired location. Using an autonomous goal-seeking algorithm, the vehicle could travel towards any number of objectives. The vehicle could be programmed to track and follow motion or travel towards an ultrasonic, radioactive, or light source. Autonomous control is the most desirable form because the device continues to be efficient and would work without any external inputs.

It is the goal of this research to implement autonomous control via a 2840 development board with PIC16F877 microcontroller to seek an ultrasonic source [22]. Though the test apparatus is bulky, it is the aim of the project to operate on the fewest number of 9-V batteries required.

After testing, the results obtained regarding the actuation of the IPMC strips, even with the additional fins, proved disappointing. However, the goal-seeking algorithm worked exactly as planned. There was some variation in the theoretical time to target from orientation to orientation due to the implementation of the algorithm, though this was an expected result. In light of the ineffectiveness of the IPMC strips as propulsors, a number of rationale were put forth to justify the fact. The addition of the fins decreased the oscillation frequency which decreased the propulsive force proportionally. In addition, to secure attachment to the vessel and fins to the IPMC strips, some of the length of the actuator had to be sacrificed.

1.7 Overview of Thesis

The first section of the thesis presents a literature survey of materials related to the research. This section also introduces the thesis.

The second portion of the thesis contains the experimental set up. This includes the description of the components involved and how they were created and assembled. The section includes the descriptions and designs of the three vessel iterations, including the sizing of the fins.

The third part of the thesis includes the controller and apparatus design. This involves the integration of the components to the 2840 board as well as the goal-seeking algorithm. This portion discusses the code and events that trigger changes in the fin operation.

The fourth segment of the thesis presents the results from the research performed. It contains information on the impotency of the IPMC fins in the case studied and the effectiveness of the goal-seeking algorithm. The section is divided in two sections, one dealing with the propulsion system and the other addressing the goal-seeking algorithm. Because the IPMC material was unable to propel the vessel a number of justifications were presented. The estimated time to target and other comparisons between different starting positions were studied.

The final portion relays the conclusions from the experiment and various generalizations and comments regarding the research performed.

2   EXPERIMENTAL SETUP

2.1 Experimental Concept

Inspired by the fish created by Eamex Corporation and guided by previous research done using IPMC material, there was a need to develop a controlled application for the material while utilizing its fin-like qualities. The prior designs using IPMC fins had no purpose or direction, as the Eamex fish only "swam" aimlessly in tanks, and other IPMC finned vessels only traveled forwards.

The vessel designed is large enough to encase a 2840 development board with the PIC16F877 microcontroller and a nine-volt battery. Three fins were connected to the back of the vessel to allow for propulsion and steering. Various goals were considered for the goal-seeking application. The first was a light-following algorithm using a light source and an array of photoresistors to track the source. The second was an ultrasonic detector mounted to the vessel to follow an ultrasonic source or both the detector and emitter mounted on the vessel to guide the vessel along a "coastline." The final goal considered was a crude positioning grid. This would be implemented using a number of light sources arranged in a grid to give relative position and one mounted to give direction. The user could enter a set of coordinates and given the current position, the vessel could travel towards the goal. Figure 2.1 depicts all three schemes.

The ultrasonic source-seeking concept was chosen in this research because it could be done without significant interference from external sources, and it was inexpensive when compared to the grid-positioning concept.
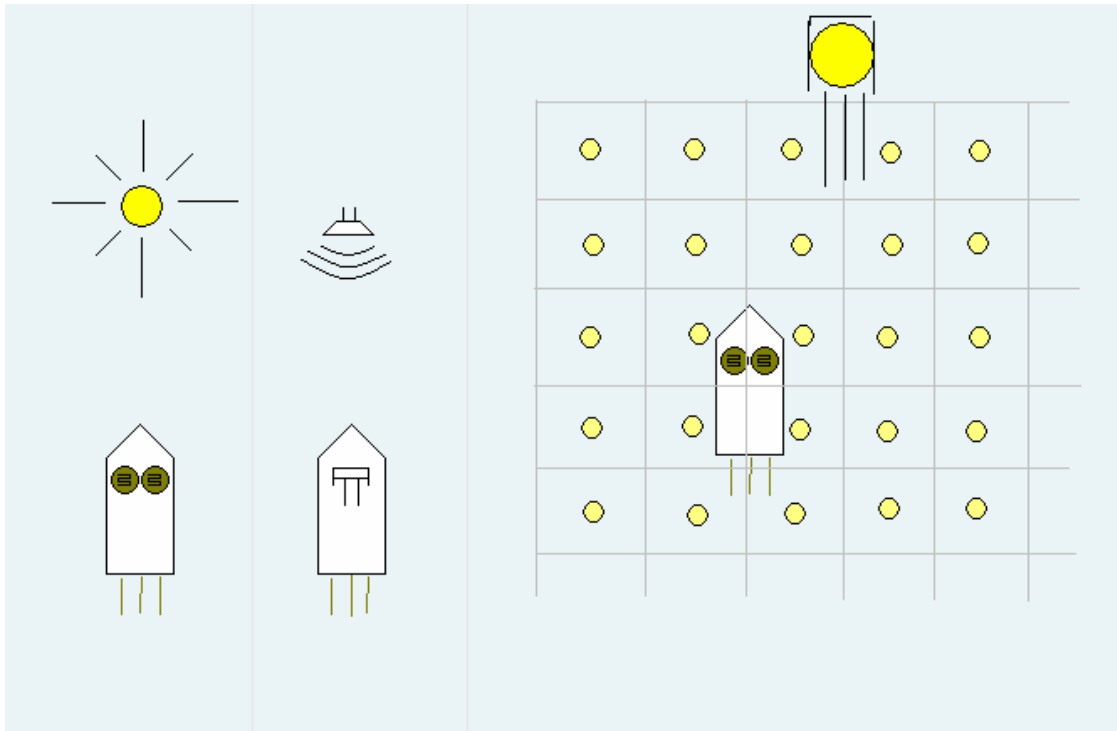
Fig. 2.1: Concepts for means of goal-seeking, from left to right: light source seeking, ultrasonic source seeking, grid positioning with direction indication

2.2 First Vessel Design

2.2.1   Constraints and Buoyancy

The first consideration while designing the vessel was to keep it afloat. Therefore it was necessary to determine how much load the vessel can carry and what dimensional constraints it must be held to. The chosen means of on-board control was the 2840 development board. This board is 3 inches by 4 inches in size and weighs approximately 80-g. A 9-V battery weighs less than 50-g. Table 2.1 shows the mass of each component involved.

TABLE 2.1: MASS OF VESSEL AND COMPONENTS

Component	Mass (g)	Quantity	Total Mass (g)
2840 Board	90	1	90
9 Volt Battery	47	2	94
Vessel*	200	1	150
Miscellaneous*	80	1	80

Vessel Mass (g): 414

* indicates estimate

With the mass of the vessel in mind, the design goal was to size the vessel large enough and deep enough so that only the bottom half would be submerged in water. It was over-designed because weight could always be added to weigh the vessel down further if needed. The gravitational force is given in (2.1),

$$F_g = mg ,$$ (2.1)

where F_g is the gravitational force, m is the vessel, and g is the acceleration due to gravity. The buoyant force, F_b can be represented as

$$F_b = V_w \cdot \rho_w \cdot g ,$$ (2.2)

where V_w is the volume of the water displaced and ρ_w is the density of water in kg/m^3. Because the desire is to over-design the vessel so that it is guaranteed to float, a factor of two is given to the gravitational force. Setting the two terms equal and solving for the vessel volume or the volume of the water displaced by the vessel gives:

$$2F_g = F_b$$
$$2mg = V_w \rho_w g$$ (2.3)
$$\frac{2m}{\rho_w} = V_w$$

Substituting in the values for the mass of the vessel and the density of water gives a desired vessel volume of 828 cm^3.

To reduce manufacturing time the vessel was created using a rapid prototyping machine that uses acrylonitrile-butadiene-styrene (ABS) plastic material. The means of creating the vessel walls could be modified to being a honeycomb-type structure rather than a solid body to reduce weight while maintaining significant strength.

2.2.2   Vessel Design and Features

The desired vessel volume was 828 m^3. The vessel was created on the rapid prototyping machine and had a volume of approximately 900 cm^3. The vessel was sized to fit the 2840 board lengthwise across the width of the vessel to allow for simpler wiring and space for the battery and miscellaneous components that were not specified at the time of the vessel creation.

The vessel was created from a *.stl* file, generated by SolidWorks, and uploaded into the controls for the rapid prototyping machine. The overall dimensions of the created vessel were 10.8 cm (4.25 inches) wide by 16.5 cm (6.5 inches) long and 5.1 cm (2 inches) deep. It was designed with a rounded nose, similar to the shape of a barge, to reduce drag. Figure 2.2 shows a side view of the vessel.
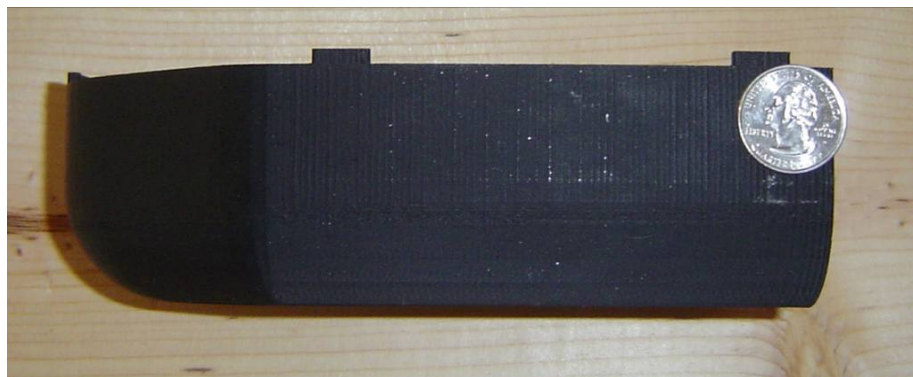
Fig. 2.2: Test vessel for IPMC fins, side view

The vessel was created in the rapid prototyping machine without any area for the placement of the IPMC fins. At the time of vessel creation, the fins were not yet cut and the electrodes were not sized at the time, so the back of the vessel was left featureless. When the electrodes and IPMC strips were specified, the fin slots were cut. Three slots, 3.2 cm (1.25 inches) apart and centered on the rear of the vessel were cut. The holes were 1.9 cm (0.75 inches) in length and cut using a 0.32 cm (0.125 inch) end mill bit. Figure 2.3 shows the slots in the rear of the vessel.
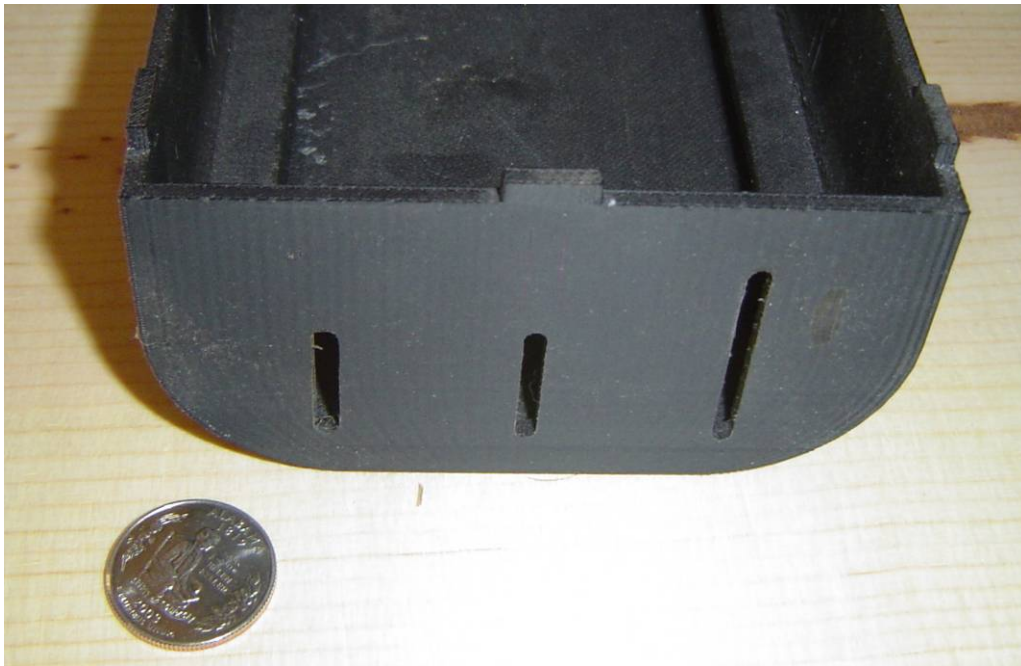
Fig. 2.3: Test vessel with slots in rear for IPMC fins and electrodes

2.2.3 Protection of Electronic Equipment

A major design consideration was that this would be an aquatic vessel carrying electronic equipment. This was one of the factors considered when over designing the

vessel for buoyant force. To protect the vessel from any splashes, a clear shield was cut

over to fit on top the vessel. This is the reason for the tabs seen in Figure 2.4.

Fig. 2.4: Close up picture of vessel showing tabs to keep water shield in place

Figure 2.5 shows the shield that was cut for the purpose of protecting the

equipment from splashes.
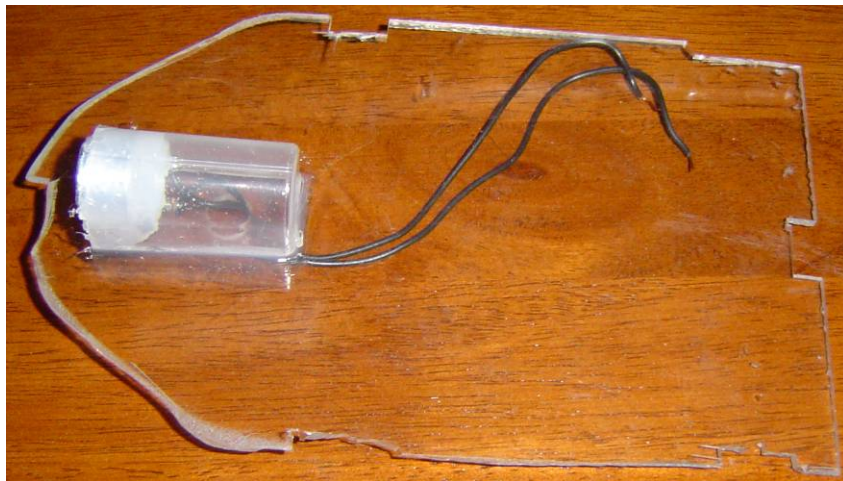
Fig. 2.5: Acrylic shield to protect electronics from water splashes made from acrylic

Due to the brittle nature of the acrylic, the shield was difficult to machine. The

shape was scored into the acrylic using a razor and carefully chipped away using a

chisel. There were a few breaks and a couple rough edges, but the shield served its

purpose.

Another design consideration was if water did somehow seep in to the vessel either by absorption through the IPMC fins or through a crack in the hull. To ensure the safety of the electronic equipment, two rails were added to the vessel design on which the 2840 board could rest. Figure 2.6 shows the rails.
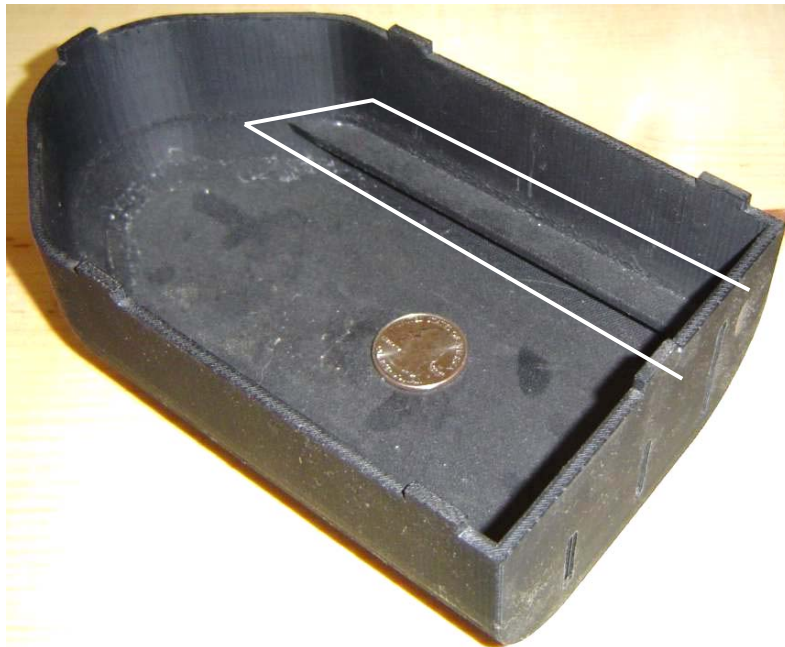
Fig. 2.6: Picture of test vessel showing railing (enclosed by white lines) to support 2840 board so it is protected from leaks in hull
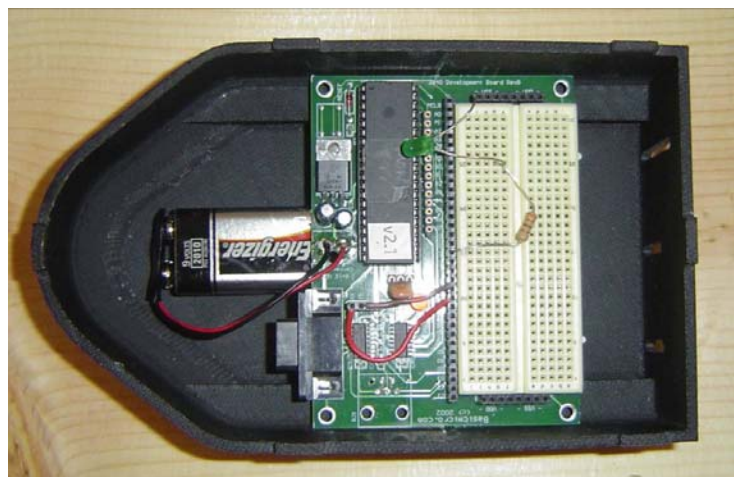
Fig. 2.7: Test vessel with major electronic components in place

The 2840 board and nine-volt battery are shown in the vessel in Figure 2.7.

2.3 Second Vessel Design

2.3.1 Vessel

The design for the second test vessel was solely focused on reducing the weight of the vessel. The previous vessel was made from a Computer Aided Design (CAD) model taking weight and volume into account to give it sufficient buoyancy. With previous experience in designing a buoyant vessel, more thought could be given to the weight reduction.

The second vessel was made from two small, 11-oz. Tupperware® containers. With a length of 9.5 cm and a width of 7 cm, this vessel was significantly smaller than the previous one. To keep the ultrasonic receiver atop the vessel, a plastic casing was used and the receiver and housing was placed on it and attached with silicone. The vessel with the receiver in place is shown in Figure 2.8.
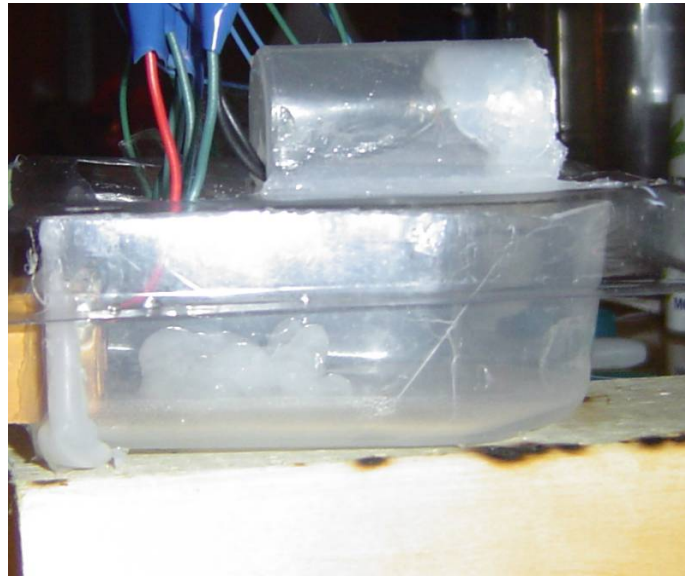
Fig. 2.8: Second test vessel with ultrasonic receiver in place

2.3.2   Communication To and From 2840 Board

Because the weight in the vessel was limited, all hardware and power that were not required to be on-board were removed and a set of umbilical cables had to be attached to the vessel. To impede movement the least, the smallest wire gauge available to the experimenter, 26 American Wire Gauge (AWG), was used. There were four devices that needed to be attached: three fins and the ultrasonic receiver. This meant eight wires had to be used. Eight 4-m wires were soldered to the leads on the vessel and in turn soldered to the leads on the 2840 board. This umbilical cable was fairly flexible, yet was considerably heavy when compared to the weight of the vessel itself.

2.4 IPMC Strip Apparatus

2.4.1   Strip Specifications

Three rectangular IPMC strips were used as actuators to propel the vessel. Due
to material restraints, the middle actuator was slightly smaller than the other two. The
exact dimensions are given in Table 2.2.

Table 2.2: Specifications of the fins

	Length (cm)	Width (cm)
Right Fin	2.7	1.7
Middle Fin	2.2	1.4
Left Fin	2.7	1.7

The three fins are all cut from the same IPMC sheet. The IPMC material used
was a Nafion 117 base polymer with chemically plated gold electrodes. This material
was provided by Virginia Tech's Center for Intelligent Materials.

2.4.2   Electrode Assembly

To actuate, a voltage must be imposed across the IPMC electrodes. Two copper
electrodes were cut for each of the fins for a total of six electrodes. All six electrodes
were cut to approximately 1.8 × 0.6 cm. One side of each electrode was polished using
200-grit sandpaper and then cleaned. This was the side that contacted the IPMC strip.
With all six strips lying on the polished side, three leads were soldered on the lower left
corner and three leads were soldered on the lower right corner.

Using insulating electrical tape, one of the electrodes in each pair was partially
covered exposing only a fraction of the polished electrode surface. The edge of the three

IPMC strips was lined up with the edge of the electrical tape on the electrode surface.

By reducing the contact with the electrode, more IPMC strip could protrude from the

vessel allowing for stronger actuation. The second electrode sandwiched the IPMC strip

in the middle of the two electrodes. Figure 2.9 depicts the assembly.

Fig. 2.9: IPMC strip assembly diagram

2.4.3   Strip Attachment to Vessel

To attach the IPMC strip assembly to the vessel, the strip and electrode assembly

was held together using a paper clip. Each of the three assemblies was inserted into the

three slots prepared. Using a silicone sealant, all gaps and holes were filled. The strips

were inserted as low as possible so full submersion would be easier. Excess silicone was

wiped off the IPMC strip and the assembly was left overnight to cure. Figure 2.10

shows a step in the process.

The edge of the copper electrode is flush to the outside edge of the vessel. The

silicone covers the electrodes to isolate them from the water.

Fig. 2.10: Middle fin held together with paper clip, attached to boat during silicone curing

2.4.4   Strip Attachment to Second Vessel

Unlike the previous design where the vessel wall thickness was considerably thicker, the edges of the electrodes could not be placed flush against the rear vessel wall. Instead, the electrodes had to jut out from the rear of the vessel. To ensure the electrodes did not contact water, substantial amounts of silicone gel were placed on them and a small portion of the IPMC strip. This resulted in the strips having slightly less effective length due to the increase in restraints. Figure 2.11 shows how the strips were attached.
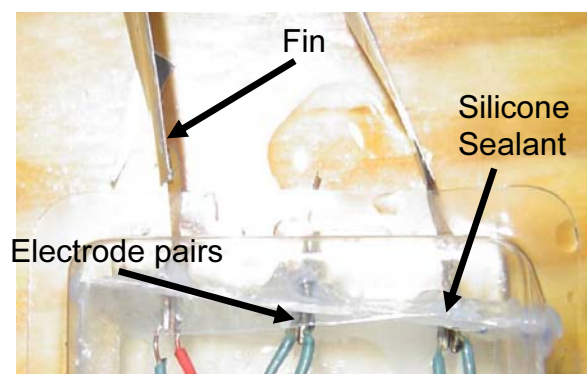
Fig. 2.11: Fin attachment to second vessel

2.5 Fin Addition

One concern that emerged from early tests with the IPMC material as well as others' research was that the IPMC strips alone would be insufficient to propel the vessel. To address this, a comparison was made between prior IPMC-propelled vessels to size a fin that could increase the propulsive force by a specific amount.

2.5.1   Fin Theory

The fins were designed so they would attach to the IPMC strips while on the second, smaller vessel. The mass of this vessel was 50.0 g, using 0.7 g of actuator material. Comparing this specific case with prior experiments such as the ray [12], tadpole [13], and snake [15] show that the actuator mass to vessel mass ratio could yield propulsion. The tadpole experiment showed that 0.05 g of IPMC could propel a 16.2 g vessel through the water, giving a mass ratio of 324. The ray and snake experiments, operating under a different propulsion principal had smaller mass ratios, of 6.4 and approximately 20, respectively. The second vessel created had a mass ratio of 71. Table 2.3 below summarizes the knowledge gained from the prior research.

TABLE 2.3: COMPARISON OF VESSEL TO ACTUATOR MASS RATIOS AND FIN SIZES FOR VARIOUS IPMC EXPERIMENTS

Experiment	IPMC Strip Mass (g)	Vessel Mass (g)	Vessel to Actuator Mass Ratio	Total Fin Area (mm^2)	Top Speed (mm/s)
Tadpole	0.05	16.2	324	1080.0	23.6
Snake	0.03*	0.6	20	N/A	8.0
Ray	1.50	9.6	6.4	625*	9.0
First Vessel	0.70	453.3	648	980.8	0.0
Second Vessel	0.70	50.0	71	700.6	0.0

* Indicates estimate

Table 2.3 clearly presents the results from three prior experiments as well as the two performed for the purpose of this thesis. Two columns, vessel to actuator mass ratio and total fin area are the most important when analyzing the use of IPMC material as actuators. Two of the experiments, the snake and ray, had vessel to actuator mass ratios on the order of 10. The two vessels created for the purpose of this thesis as well as the tadpole experiment had vessel to actuator mass ratios on the order of 100 and 1000. The tadpole was autonomous and had no umbilical wires or power sources. Its power cell was carried onboard, but no control other than driving frequency was given. One noticeable addition to the tadpole was a large fin. This fin was roughly 1000 mm^2 in area, increasing the propulsive power of the tadpole significantly.

Comparing the tadpole fin surface area to the total fin surface area of the three fins on the vessels prepared for the experiments performed for this thesis gives a surface area of 980.8 mm^2 for the first vessel and when taking effective fin length into account, approximately 700 mm^2 for the second vessel. Comparing these three experiments shows that a larger fin size may be helpful in moving any vessel through the water.

One notable observation was the top speed obtained in each of the three experiments. The speed in any direction was on the order of 10 mm/s, or 0.022 mph. This speed is virtually negligible. To move through the entire 2 m range of the ultrasonic transmitter would take around 3 minutes with the fastest IPMC motor.

This table shows that both vessels from this research were "overweight" when compared to the other three. However, the second vessel and the tadpole were comparable when it came to vessel mass and the vessel to actuator mass ratio was below

what was given for the tadpole. The striking difference is the total fin area between the two vessels. Weighing only a third of the amount of the second vessel created, the tadpole had about 50% more fin area, though not all of this was actuator material; some was actually a static sheet of plastic attached to the fins. To scale the tadpole experiment up three-fold to compare it to the second vessel created would give comparable vessel masses, yet it would only have 20% of the actuator mass. The fin size would increase threefold as well, giving it about 350% more fin area than the second vessel created. From this comparison, it can be concluded that the reason either vessel was unable to move is the lack of fin size.

A few concerns regarding the attachment of fins were attended to and considered. First, a decrease in actuator performance due to the added load was an issue. Secondly, there was a concern that the attachment method could possibly damage the IPMC material as prior research had not indicated a proper means of attachment. Finally, there was the issue of the fin attachment requiring a lot of IPMC material to be covered so that it would be attached securely.

To size a fin, Rosen [23] gives a number of equations that describe the propulsion caused by an oscillating fin. In Rosen's paper, he introduced his "Vortex Peg Hypothesis" which states a fish propels itself by pushing off of vortices created by the oscillations of its tail fin and body. He developed an equation for the mass of the vortex created due to the stroke of the tail:

$$m = \frac{Lbwh}{g},$$
(2.4)

where *m* is the mass of the vortex, *L* is the length of the fish, *b* is the height of the

tail, *w* is the weight density, *h* is the half-thickness of the fish, and *g* is the gravitational

acceleration. Rosen then made the assumption that the amplitude *a* of the tail fin's

motion is equivalent to the length *L* of the fish. In one tail fin stroke, the force *F*

imparted in the forward direction by the fish is proportional to the geometry of the fish,

shown by (2.5):

$$F \propto \frac{abhw}{g}.$$

(2.5)

Therefore to increase the force generated by a fin stroke, the fish geometry must

increase. An additional fin-shaped attachment to the end of the IPMC strip, as shown in

Figure 2.12 should suffice.
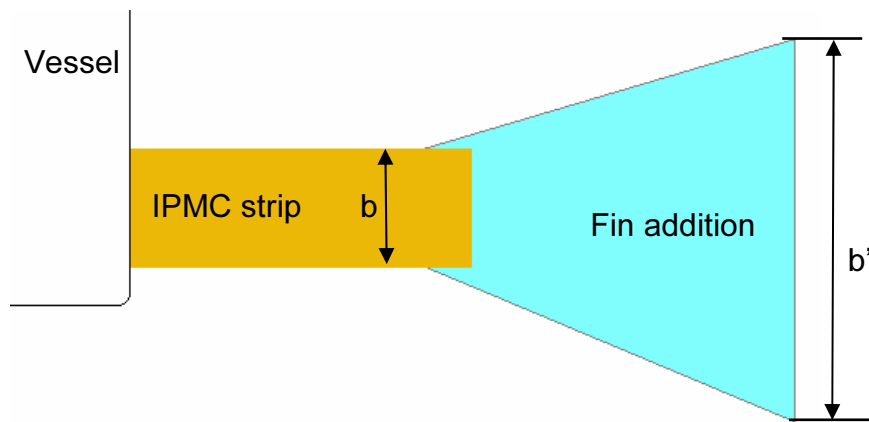
Fig. 2.12: Fin addition to IPMC strip, side view

Figure 2.13 shows the top view of what the fin addition would look like. The

amplitude of oscillation, *a*, is shown, and it increases as the strip length, *b* increases.

Assuming a 30° maximum deflection angle of the fin, and the 2.7-cm length and 1.7-cm

width as used in the experiments, and an approximate tip deflection of 0.7 cm, the

dimensions indicated are shown in Table 2.4.
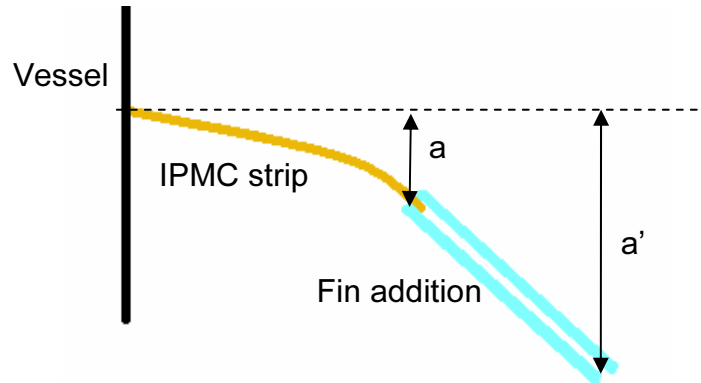
Fig. 2.13: Fin addition to IPMC strip, top view

TABLE 2.4: TABLE OF FIN AND IPMC STRIP DIMENSIONS

Dimension	Value (cm)
a	0.7
A'	0.7+0.58×l
B	1.7
B'	z

In Table 2.4, l and z are the dimensions of the fin, length and height, respectively.

Comparing the two forces, with and without additional fins gives (2.6):

$$F \propto \frac{0.7 \times 1.7 hw}{g}$$
$$F' \propto \frac{(0.7 + 0.58l)zhw}{g}$$

(2.6)

All other parameters being equal,

$$\frac{F}{c} \propto 1.19$$
$$\frac{F'}{c} \propto (0.7 + 0.58l)z$$

(2.7)

From (2.7), it can be shown how increasing the dimensions of the fin affect the propulsive force generated. This phenomenon is depicted in Figure 2.14, created by dividing the proportional force factor $\dfrac{F'}{c}$, due to the addition of a fin, by the current proportional force factor, $\dfrac{F}{c}$.
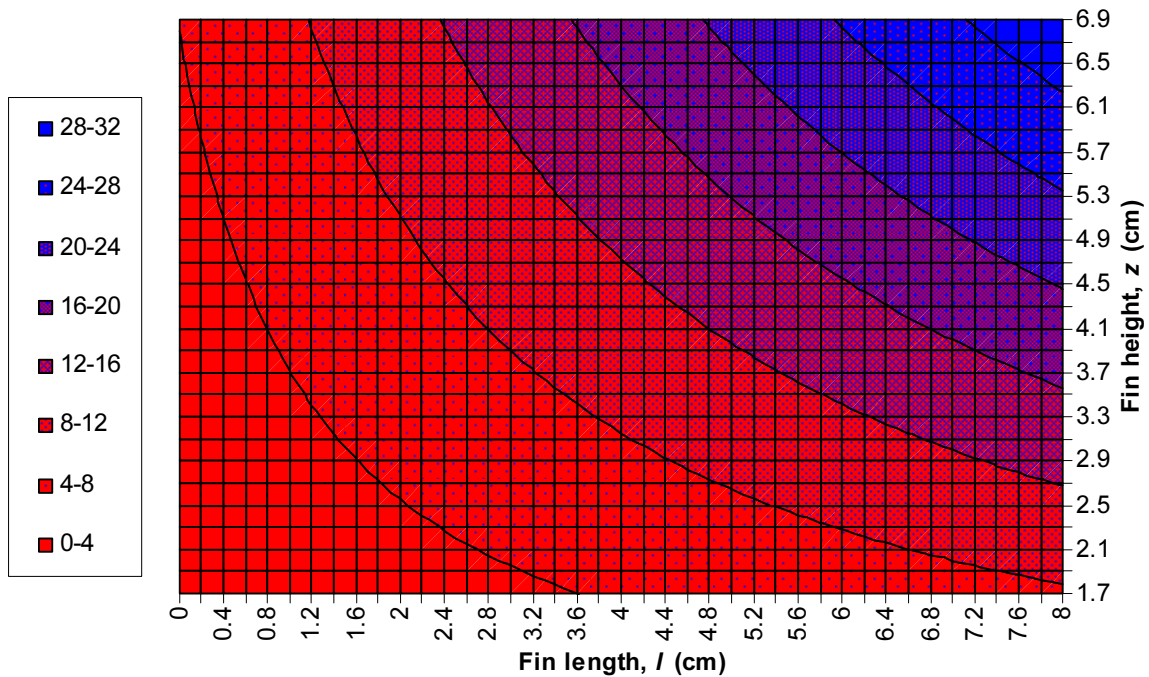
Fig. 2.14: Proportional increase in propulsive force as a function of fin dimensions

Figure 2.14 shows how increasing the fin size over the current fin size results in an increase in propulsive force. The bottom left corner represents the IPMC strip without any additional fin. Given that the second vessel's fin surface area is 700.6 mm^2, and to match the tadpole experiment would require an increase in this fin area by 350%, a total fin area of approximately 2500 mm^2 would be needed to propel the second vessel, an additional fin with a size of 1800 mm^2. Depending on the geometry used to achieve

this increase in fin size, the increase in force could be as little as 10 to as great as 13 times the propulsive force imparted by an IPMC strip alone. By increasing the fin height to 2.3 cm and the fin length to 8 cm gives a 10-fold increase in propulsive force. On the other hand, increasing the fin height to 6.7 cm and the fin length to 2.8 cm gives a 13-fold increase in propulsive force.

2.5.2   Fin Specifications

The fins were made from a thin plastic film, cut from overhead transparencies. This plastic was easy to cut, readily available, and light weight. Each of the three fins was cut to the same size and a short extension was added to the end of the fin to give some area on which the adhesive could be applied. Figure 2.15 shows the dimensions of the fin.
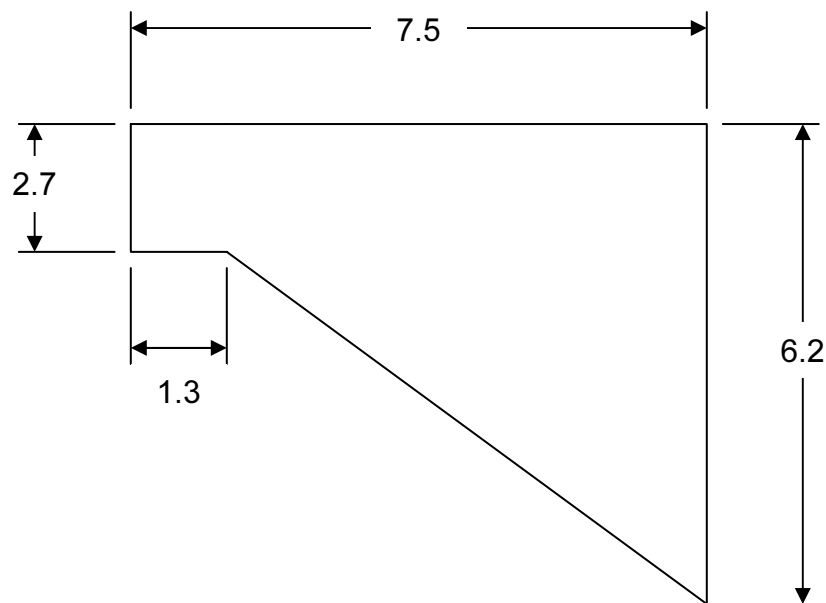
Fig. 2.15: Dimensions of fin addition in centimeters

Excluding the tab used for the adhesive, the area of the fin is 32.6 cm^2. From Rosen's equations, this represents a 22.4-fold increase in force, from the height and length of the fin. While the desired 350% increase in fin area determined from the scaling of the tadpole experiment would yield a 10 to 13-fold increase in force, the 737% increase in fin area introduced by the plastic fin gives a 22.4-fold increase in propulsive force. This doubling of the necessary fin size was done to further increase the propulsive force and make it easier for the vessel to turn since only one fin is acting in that case. Figure 2.16 shows the fins on the vessel, attached to the IPMC strips.

Fig. 2.16: Fins attached to IPMC strips with epoxy resin

Using commercially available epoxy resin, the fins were attached to the vessel. Initially, the fins were cut and folded over on themselves. When the IPMC strips were tested in the water with the doubled over fin, no actuation at all was observed so the fins were cut in half, sacrificing some thickness and rigidity, but allowing for actuation. With the fins attached and actuating properly, they could be tuned to an optimal operating frequency and used for propulsion.

2.6 Ultrasonic Components

To direct the vessel, an ultrasonic transmitter/receiver pair was used. The receiver was placed on the vessel, and the transmitter was placed in a project box away from the vessel. Using part of a plastic case from a candy container for its encasement, the receiver was positioned within the plastic case as seen in Figure 2.17.

Fig. 2.17: Ultrasonic receiver encased atop the acrylic shield, sealed with silicone

Two wire leads were soldered onto the receiver leads and guided through a hole drilled in the acrylic. The receiver assembly was positioned on the top of the acrylic shield and sealed using silicone. The ultrasonic transmitter was placed in a plastic project box and sealed using the same means as the receiver.

The ultrasonic transmitter and receiver operate optimally at a frequency of 40 kHz. This is the frequency at which the receiver is most sensitive. The data sheet for the ultrasonic pair gives a sensitivity of approximately –60 dB. Because it is so low, the received signal must be amplified so that the microcontroller can read it.

3 ELECTRICAL COMPONENT DESIGN

3.1 Electrical Component Concept

To guide the IPMC propelled vessel towards a specific location, some control algorithm must be used to ensure it reaches its target. To implement this system, three things are required: a target that can be detected, a means to detect that target, and a means to get there. To detect the target, an ultrasonic transmitter will be placed on it. The ultrasonic waves produced by the transmitter will be received by an ultrasonic receiver on board the vessel. After the signal is processed, it will be read by the microcontroller, and the goal-seeking algorithm will be employed to drive the vessel towards the target.

When the transmitter circuit is designed for optimal results, the transmitted wave must be as close to 40-kHz as possible because this is the frequency at which the receiver attenuates the signal the least, according to the ultrasonic component data sheet. To help alleviate the problem with attenuation, the amplitude of the generated wave must be as high as possible, as close to the upper limit of the operating voltage range of the transmitter as possible.

To process the sinusoidal output of the ultrasonic receiver so it can be read by the microcontroller requires a number of signal processing techniques. The microcontroller is only able to read signals from 0 to 5-V, giving a need for rectification. Due to the attenuation of the signal between the transmitter and the receiver there must be a significant amount of amplification. For the microcontroller to read the amplitude of the

signal, it should ideally be a constant value, giving a need for a low-pass filter to produce a DC signal that can be read by the microcontroller.

To drive the vessel to the goal, the three IPMC strips must be "told" what to do by the microcontroller based on the signal received. The vessel should seek the highest voltage, orient itself in that direction, and travel there. The algorithm should allow for periodic detections to ensure the vessel stays on target. To move the vessel, the output to the fins must have enough current to actuate them yet not exceed the ideal driving voltage.

3.2 Transmitter Circuit

To produce a signal that can be read by the receiver, an ultrasonic transmitter was used. The manufacturer's model number of the transmitter was 400ST160 from Ceramic Transducer Design Co. Ltd based in Taiwan[1]. This transmitter receives a voltage signal and outputs a pressure wave.

Various means to achieve the 40 kHz frequency were considered. One concept was to use a microcontroller to generate a square wave with the desired frequency. This would require amplification to achieve a voltage within the operating range of the transmitter and the period of the signal borders on the computing time limitations of the microcontroller. A second idea was to use a 40-kHz oscillating crystal. This concept was not used because it was difficult to find clear documentation on the specifications of individual crystals. The idea chosen to drive the transmitter circuit was to use a 555

---

[1] Datasheet available online through vendor's website at
http://info.hobbyengineering.com/specs/t400s16.pdf

timer, operating in astable mode. The operating voltage of the 555 timer ranges from 5

to 20 V, and the frequency and duty cycle of the signal can be tuned by changing

resistaces in the circuit.

  With the design for the 555 timer operating in astable mode, a potentiomenter, or

variable resister, was placed where R_A and R_B belonged. The capacitor C_D is set to 0.01

μF and C was picked to be 10 nF. Figure 3.1 shows the circuit for the astable operation

of the 555 timer[2].
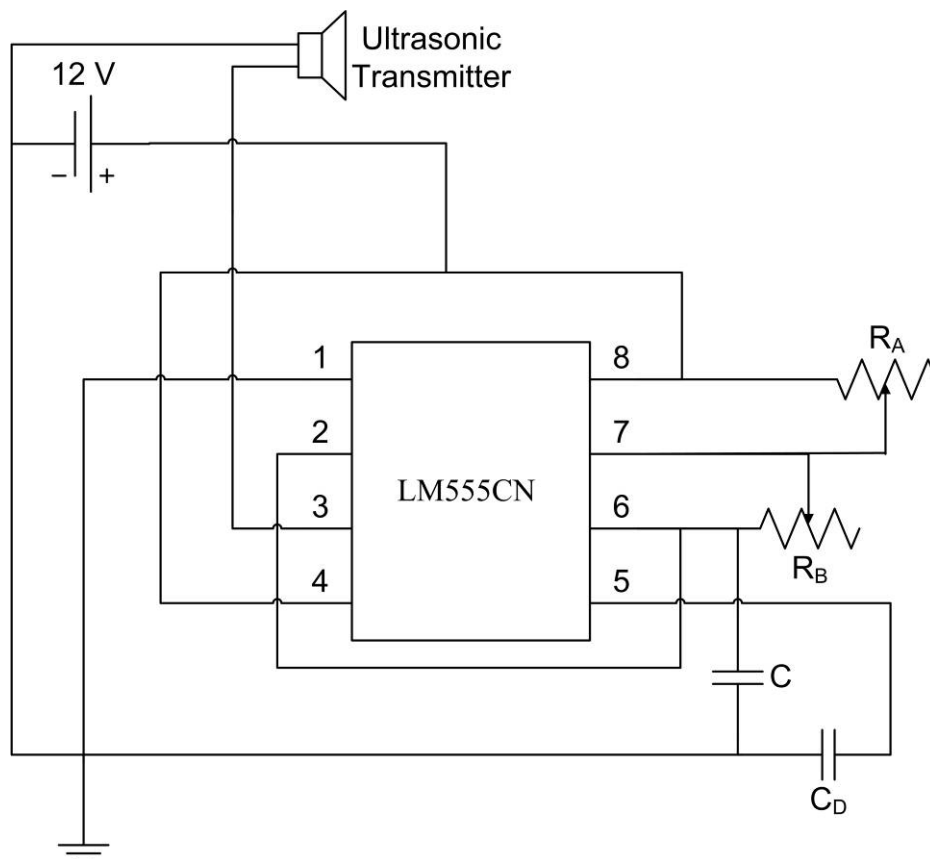
Fig. 3.1: Circuit diagram for 555 timer working in astable mode connected to the ultrasonic transmitter

---

[2] Datasheet available online through vendor's website at
http://www.alliedelec.com/Images/Products/Datasheets/BM/TEXAS_INSTRUMENTS/Texas-
Instruments_Actives-and-Passives_7350875.pdf

Given the capacitor and that a frequency of 40 kHz was desired, the following

design equation was used to size the trimmers, from the 555 timer data sheet.

$$f = \frac{1.44}{(R_A + 2R_B)C} \qquad (3.1)$$

Substituting in the values for f, frequency and C and solving for $R_A + 2R_B$:

$$40000 = \frac{1.44}{(R_A + 2R_B)1 \times 10^{-9}} \qquad (3.2)$$

$$0.00004(R_A + 2R_B) = 1.44 \qquad (3.3)$$

$$(R_A + 2R_B) = 36000. \qquad (3.4)$$

By (3.4), it is evident that at least one potentiometer must be able to exceed 10

kΩ, and according to the equation for duty cycle of the generated square wave:

$$D = \frac{R_B}{(R_A + 2R_B)} \approx 50\% \qquad (3.5)$$

The values should be about the same order of magnitude if the duty cycle is to be

kept close to 50%. Using a 12 V supply from 8 AA batteries connected in parallel, the

circuit is created and connected to the ultrasonic transmitter. Using an oscilloscope, the

frequency is tuned to the desired 40 kHz by turning the potentiometers, and the circuit is

soldered onto a development board and placed into a project box as seen in Figure 3.2.
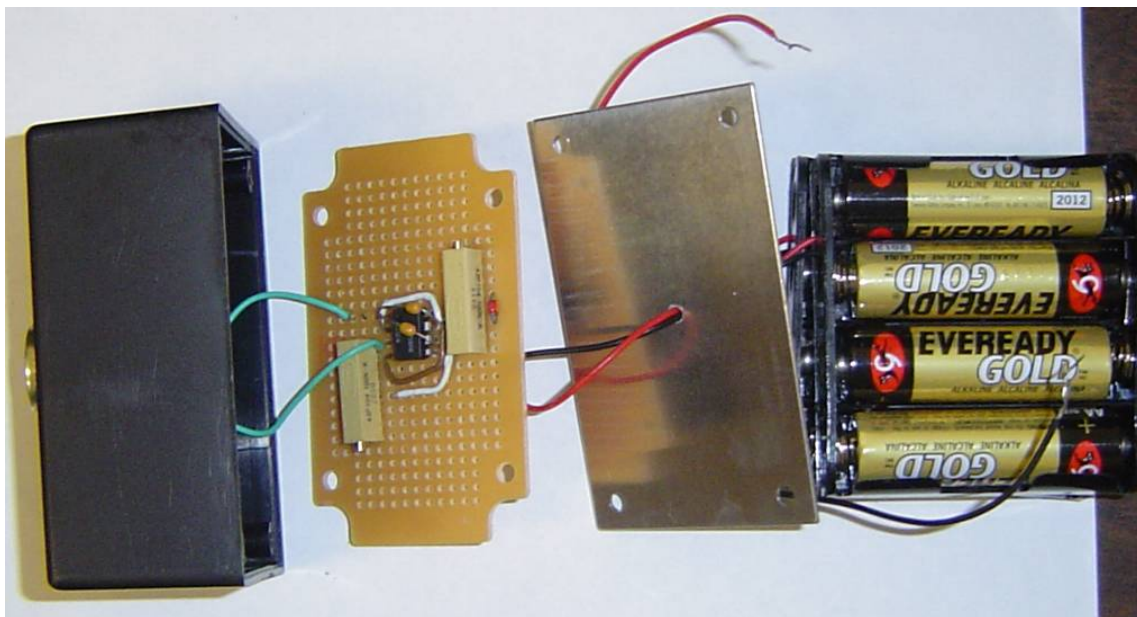
Fig. 3.2: Transmitter circuit, with (from left to right) ultrasonic transmitter encased in project box, 555 timer astable circuit, base of project box, and 12-V power supply

3.3 Receiver Circuit

To process the 40-kHz sinusoidal signal received by the ultrasonic receiver from the transmitter, it must be rectified, amplified, and filtered. These three operations would require diodes, an operational amplifier, and a capacitor. To determine the gain factor and develop an accurate profile of what signal is received at specific locations and orientations, a number of tests were conducted to produce an area mapping of voltage output from the receiver. The transmitter was moved around a grid with 30 cm spacing at orientations parallel and at 45° to the receiver. The amplitude of the receiver signal was measured through an oscilloscope. Figures 3.3 and 3.4 depict the test method used to generate the data.
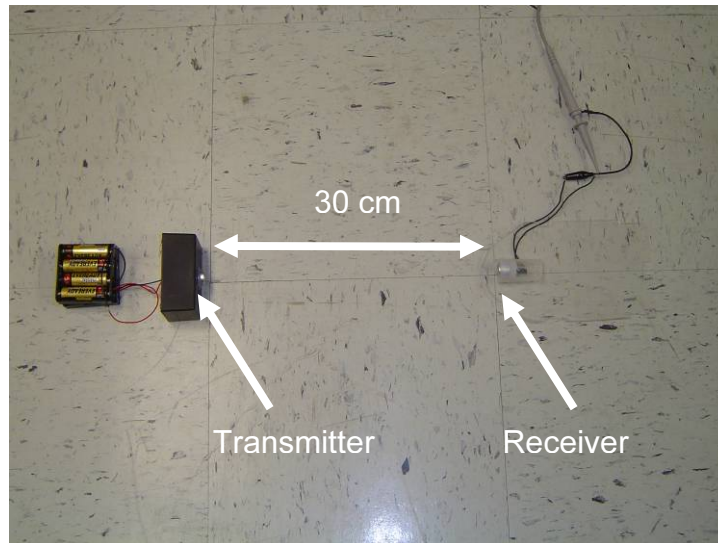
Fig. 3.3: Testing voltage output from receiver
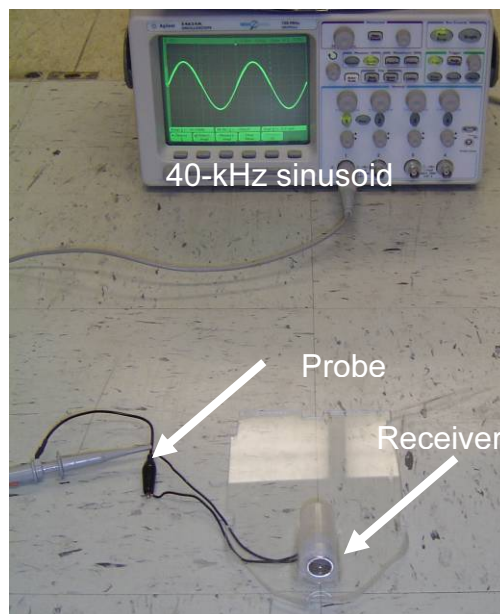
Fig. 3.4: Test in progress showing receiver output on oscilloscope

Recording the peak to peak amplitude from the oscilloscope as the transmitter is moved from position to position gave the following voltage profiles as functions of location.
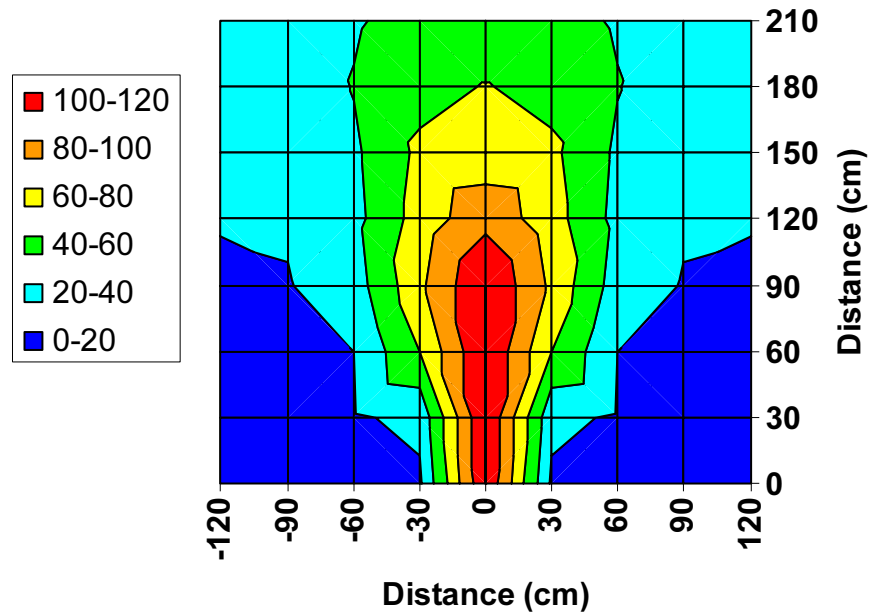
Fig. 3.5: Voltage profile from receiver with transmitter parallel to the receiver
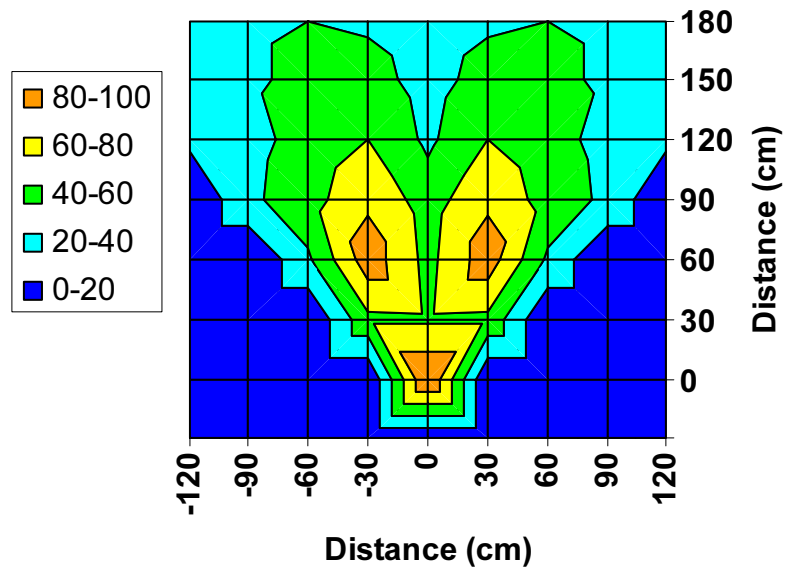
Fig. 3.6: Voltage profile from receiver with transmitter oriented 45° towards receiver

The symmetry in Figures 3.5 and 3.6 is because the data was copied about the

receiver's axis after a number of data points on the opposite side of the axis were

confirmed to be within the precision of the measurements, which was determined to be

±10 mV. Not only will this data help determine guidelines for the goal-seeking

algorithm, but will also aid in determining signal processing needs.

To obtain a purely positive signal, a half-wave rectifier is implemented by using

a circuit with diodes, allowing current to pass in only one direction. When using a real

diode to rectify, there is a bias voltage of 0.7 V that the signal must overcome to work

properly. When dealing with a small signal on the order of millivolts, as outputted by

the receiver, a real diode would not suffice. To create an ideal diode requires the use of

a powered device to overcome the bias. The circuit required two diodes and an

operational amplifier (op-amp). Picking resistor values at the op-amp inputs and

feedback loop allows for simultaneous signal amplification. To generate a near-DC

signal, it is passed through a low-pass filter with a cut-off frequency around two orders

of magnitude less than that of the signal frequency. Figures 3.7 through 3.9 show the

signal processing steps.
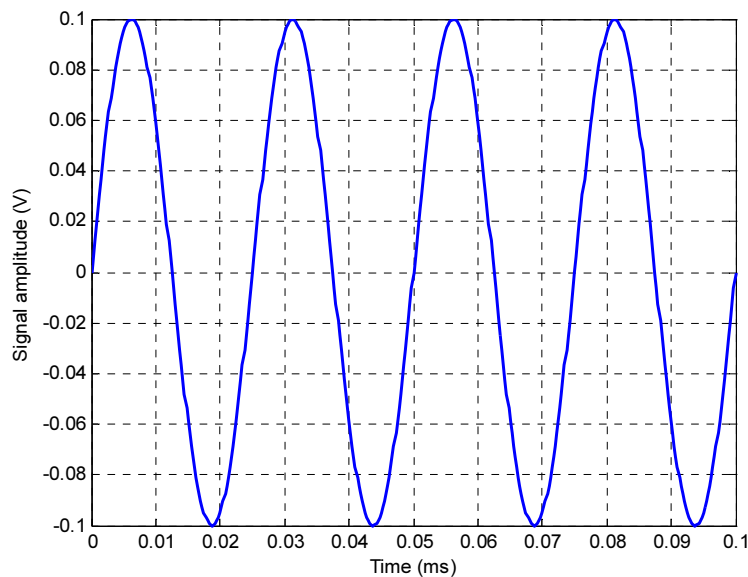
Fig. 3.7: 40-kHz sinusoidal signal generated by ultrasonic receiver
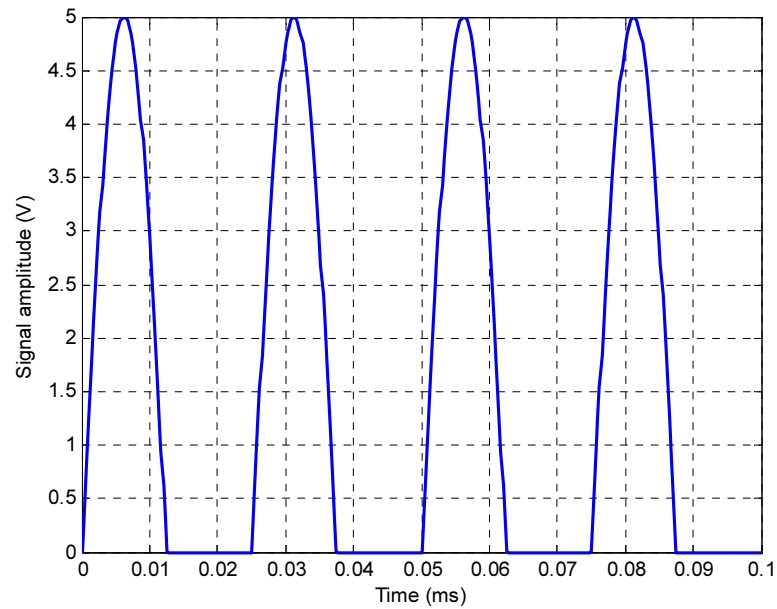
Fig. 3.8: Rectified and amplified signal after being passed through the ideal half-wave rectifier circuit
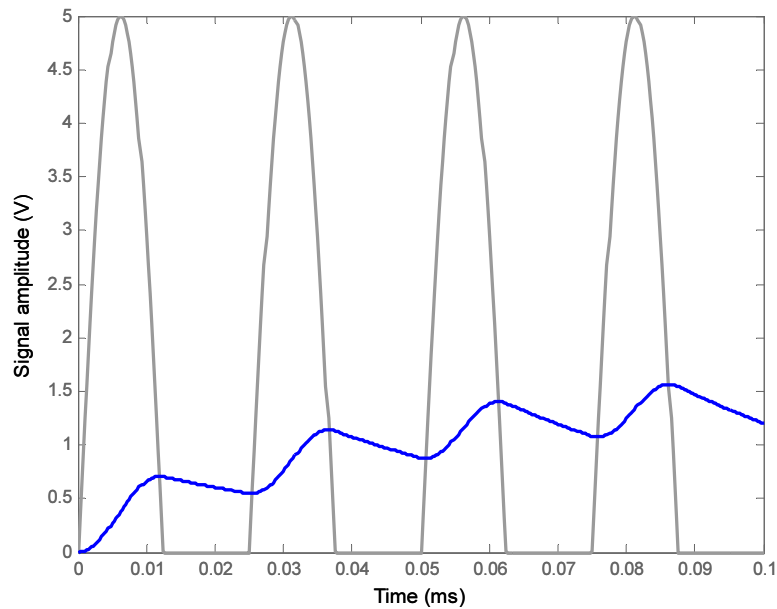
Fig. 3.9: Filtered signal to obtain a measurable amplitude (superimposed over rectified signal)

The circuit outputted to port A0 on the PIC 16F877 microcontroller so the analog signal could be measured by the microcontroller. Figure 3.10 diagrams the circuit used.
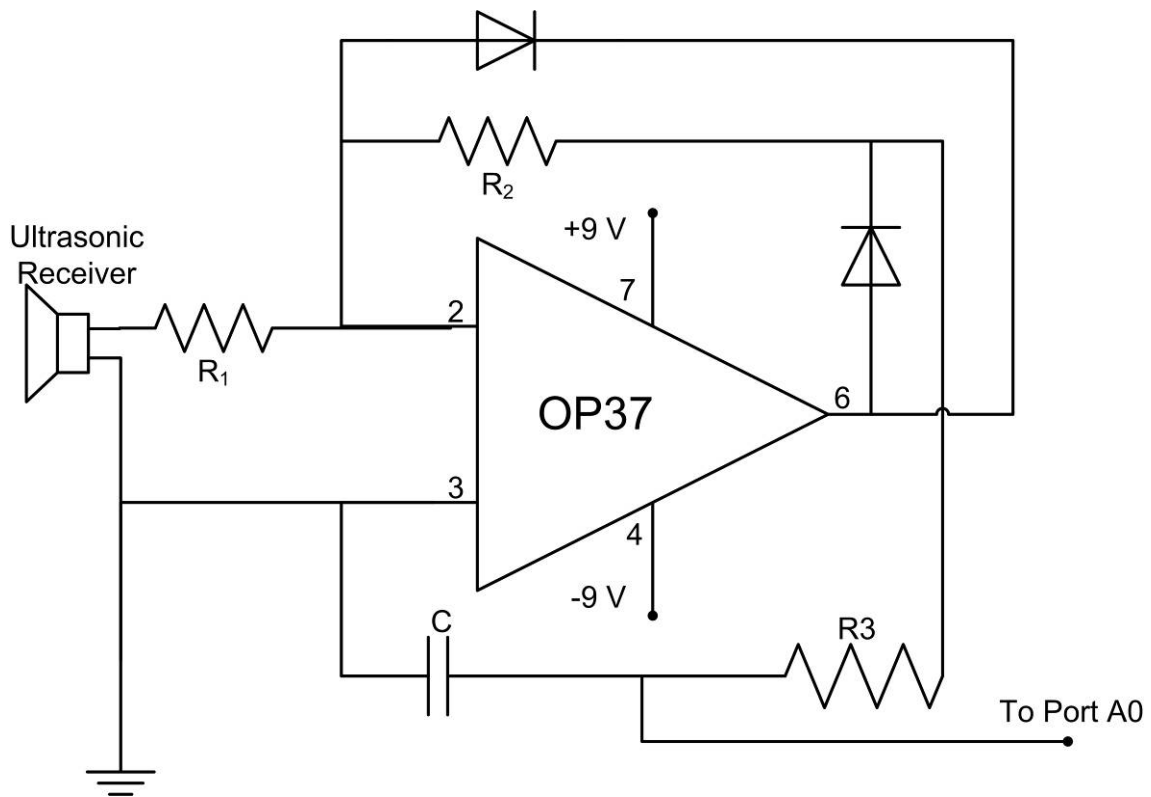
Fig. 3.10: Circuit diagram for ultrasonic signal processing

The op-amp, OP37 was chosen over others because it produces little noise and is intended for high frequency signals due to its slew rate of 17 V/μs, allowing it to accurately recreate the 40-kHz signal that is sent to it. The resistor values were selected according to the design equations of an inverting op-amp.

$$\text{Gain} = \frac{R_2}{R_1} \qquad\qquad (3.6)$$

The two resistor values were first chosen so that the gain was approximately 50. However, after the theoretical output of an RC filter (Figure 3.7) was reviewed, the gain was increased so the full range of the microcontroller's analog reading ability could be

utilized. To determine the cut-off frequency of the low-pass filter, the following relation was used:

$$\omega_C = \frac{1}{2RC\pi} \qquad (3.7)$$

To set the cut-off frequency close to two orders of magnitude less than 40-kHz, or around 0.4-kHz, a capacitor value of 1.0 µF was used with a resistor of 1 kΩ, giving a cutoff frequency of 1.57-kHz.

3.4 Driving Circuit

In order to supply sufficient power to the IPMC strips some amplifying circuit must be used. Two options were available for this purpose: a Darlington pair and an H-bridge circuit. Both would work to supply greater power to the IPMC fins, yet some consideration had to go into how each amplifying circuit works.

The Darlington pair, commonly found in the chip ULN2003, works by having one common node as the supply voltage and the outputs controlled by the microchip logic as grounds when necessary. To use this circuit to supply some positive voltage to one electrode with the remaining electrode as ground and then reverse them to bend the IPMC in the opposite direction is impossible. Therefore, the H-bridge was utilized. The package used was the L298HN, which contains two H-bridge circuits. It can supply a high voltage in binary form (high and low) at the output and is commonly used in DC-motor drivers where operation is required in both directions. Therefore, the logic supplied to the inputs is then, in turn supplied to the outputs at the desired driving

voltage. The voltage source used to drive the circuit was a 9-V battery. Figure 3.11 shows how the electrodes were connected to two L298HN.
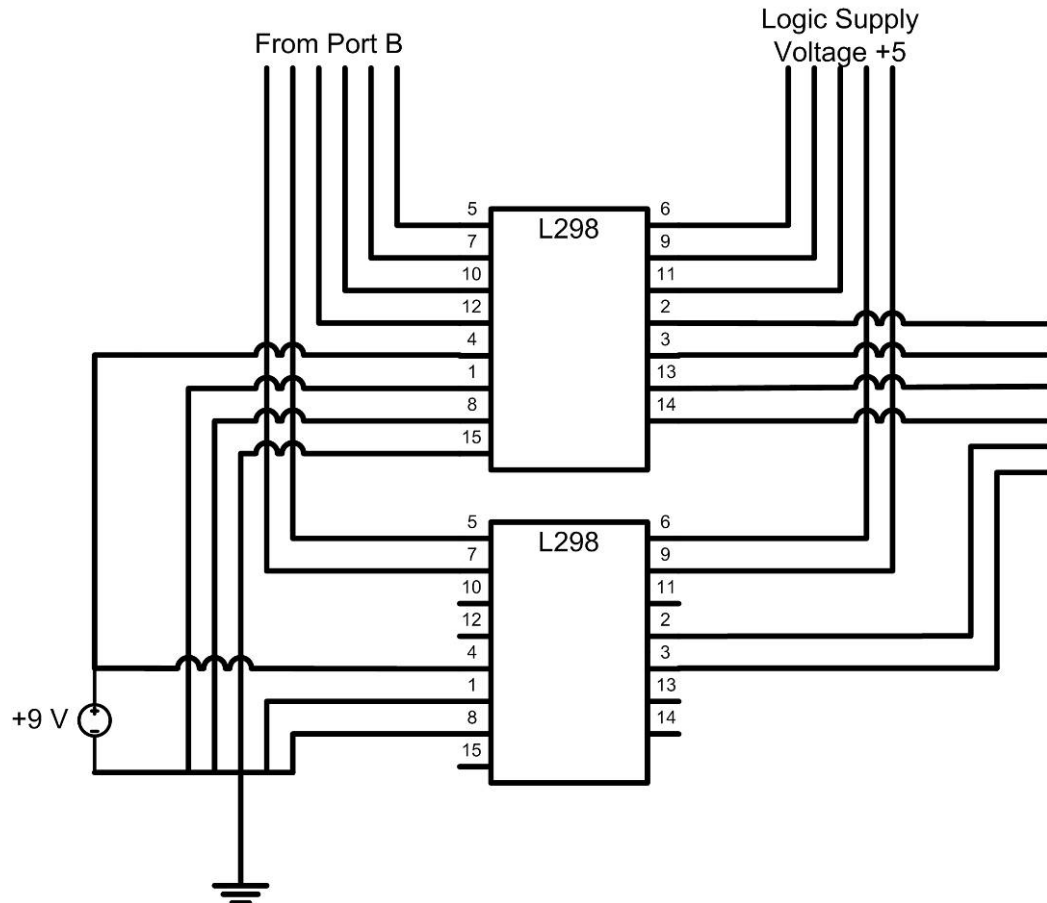
Fig. 3.11: L298HN connection diagram

3.5 Controller Algorithm

The vessel was directed to the goal by an algorithm written in C and uploaded into the microcontroller. A few algorithms were considered that told the vessel to operate very differently. The first algorithm considered instructed the vessel to rotate in a full circle, determine the location of the strongest signal, and return to that position. The second algorithm examined was one that told the vessel to measure the ultrasonic

signal, turn one direction and measure the signal strength again. It would then instruct the vessel to go forward or turn back on itself and go forward, depending on which signal was the strongest. The third algorithm was similar to the second, but after turning one direction it would turn twice in the opposite direction and take a measurement. The vessel would then be told to turn or travel forward due to the strongest signal. The goal-seeking algorithm that was chosen was the third algorithm. If the strongest signal was on the wrong side of the vessel, both would require the vessel to turn in a circle before reading the strongest ultrasonic signal.

To accomplish the task of designing the selected algorithm, the C code (located in Appendix B.1) was broken up into five parts. Four were user defined functions, and the remaining part was the main code. Of the four user defined functions, one defined a means to read the analog signal from the ultrasonic receiver. The other three instructed the vessel to turn right, turn left, and go forward. These four functions are embedded in the C code.

To read the analog signal, the microcontroller was instructed to read the voltage at port A0 and store it as a variable. This function was called "`read`." It only required two lines of code and was very straight forward.

The three functions to command the fins to propel the vessel were named "`left`," "`right`," and "`forward`." The algorithm for each of these was very similar, save for one part. The only difference was the instruction as to which fins did what. To turn left, the right-most fin must oscillate. To turn right, the left-most fin must oscillate. To go forward quickest, all fins should oscillate. Placing the controller for the right fin's

right electrode at pin B0 on the microcontroller and ending with the controller for the left

fin's left electrode at pin B7. While testing the microcontroller, ports B1 and B2 were

not reaching their "on" state. Instead of the desired 5-V to activate the H-bridge driver,

the voltage read on these ports was on the order of 1 to 3-V. Due to the aforementioned

technical difficulties with ports B1 and B2, they were both skipped to ensure proper

output from all necessary bits. Table 3.1 shows the pin designations.

Table 3.1: Pin designations for IPMC fins on microcontroller

Fin	Electrode	Pin
Right	Right	B0
Right	Left	B3
Center	Right	B4
Center	Left	B5
Left	Right	B6
Left	Left	B7

To instruct a number of fins to actuate in one line of code, the hexadecimal or

binary equivalent can be used. To propel forward, with all fins actuating back and forth,

pins B0, B4, and B6 should be high, then pins B3, B5, and B7. The output byte on port

B for the first case is 0101 0001. The second case is 1010 1000. Translating into

hexadecimal for a more efficient code gives 51 and a8 respectively. Table 3.2

summarizes the hexadecimal equivalent for each fin instruction.

Table 3.2: Hexadecimal fin commands

Command	Fin Direction	Hexadecimal
Forward	Right	51
Forward	Left	a8
Right	Right	40
Right	Left	80
Left	Right	01
Left	Left	08

The actual algorithm implemented for each fin included a simple PWM code, within the C code, to adjust the voltage going to the fins. This part sent a voltage to the electrodes specified by Table 3.2 and turns it off a number of times to actuate the fin in one direction. After the fin is fully actuated, all outputs are set to zero so the fin returns to its neutral position. A second PWM code is then performed in the reverse direction. Figure 3.12 shows a flow chart for the PWM algorithm, which only repeats a certain number of times before it stops. Figure 3.13 shows the flow chart to move the vessel.
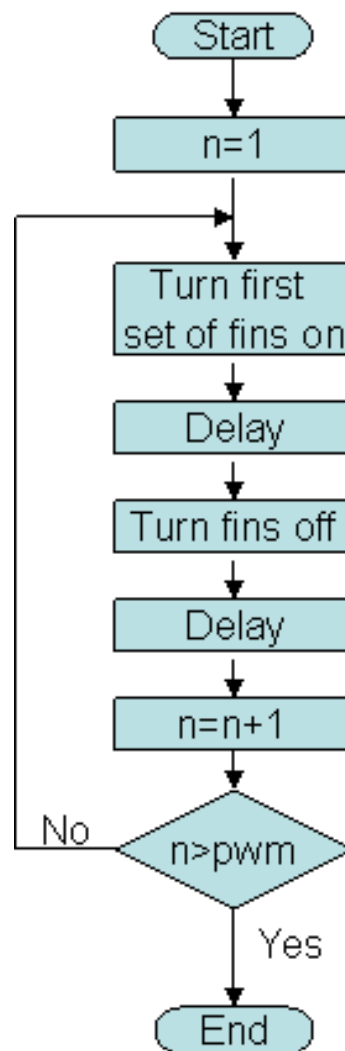
Fig. 3.12: PWM algorithm to actuate fins in a certain direction
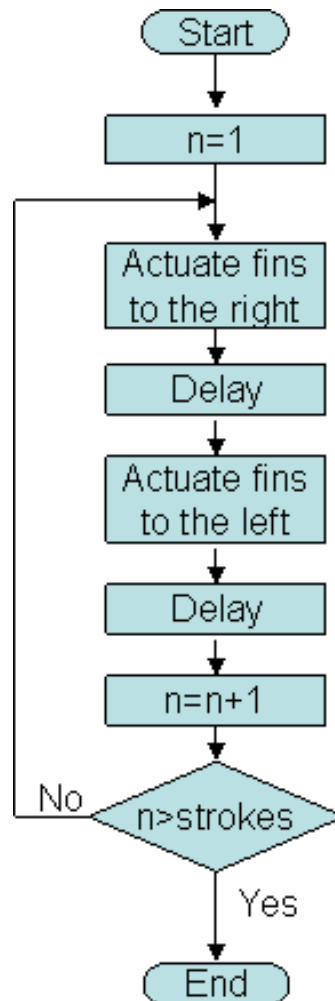
Fig. 3.13: Generalized algorithm for a certain number of strokes in any direction

The two algorithms aforementioned are used to define the three motions of the vessel: forward, left, and right, depending on which hexadecimal number from Table 3.2 is inserted into the code to apply certain voltages on port B.

To approach the goal, a fairly simple algorithm was conceived. As long as the voltage read by the ultrasonic transducer is less than some threshold, normal vessel operation will continue, seeking a stronger and stronger signal. To initialize, a variable called *value*, which is used to store the byte received on port A0 in decimal format, is

initialized to zero. The threshold value, *th*, is set to some desired number, less than or

equal to 255, the greatest decimal value of any byte. Within a while loop designed to

stop when the value read on port A0 is exceeds the threshold *th* is the driving algorithm.

First, the analog value from port A0 is read and stored as *V0*. The vessel is then

instructed to turn right by actuating the left fins according to the algorithms and

necessary logic outputs aforementioned. The analog value is read again and stored as

V1. The two values obtained from port A0, *V0* and *V1*, are then compared. If *V1* is

greater than *V0*, the C code instructs the vessel to move forward and read the value on

port A0 once again before reaching the end of the while loop. If *V1* is less than *V0,* this

means the vessel is traveling in the wrong direction and the code instructs the vessel to

turn back left two times the distance it turned right. Port A0 is sampled again and stored

as *V1*. If *V1* is greater than *V0*, the vessel is instructed to move forward and read the

value on port A0. If not, the code dictates the vessel should turn back to the right to its

initial position, where it started at the beginning of the while loop, then move forward

and sample port A0. Figure 3.14 contains the flow chart for the goal-seeking algorithm

used.
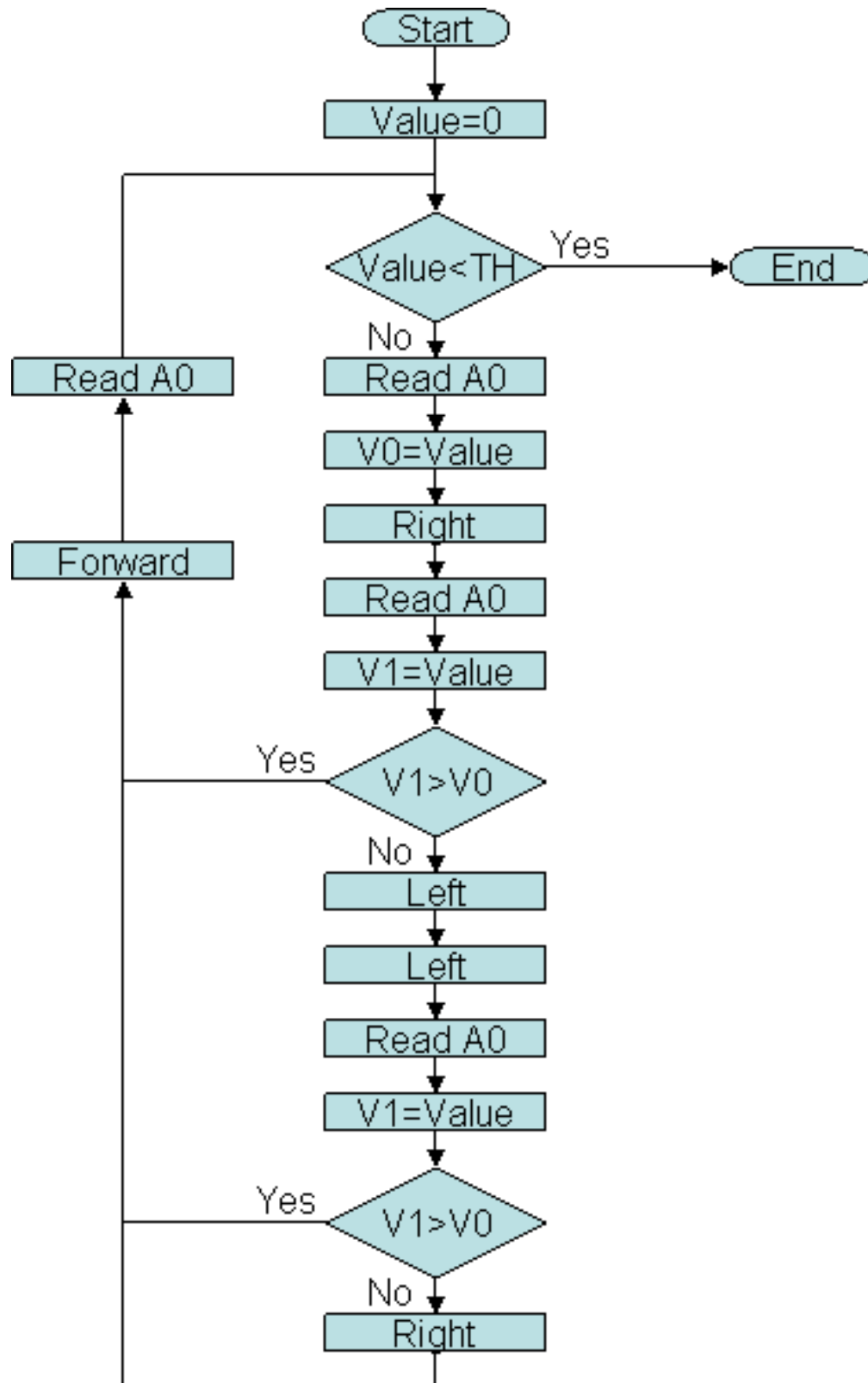
Fig. 3.14: Flow chart for goal-seeking algorithm

4   EXPERIMENTAL RESULTS

A series of experiments were performed to test the both the propulsion and the ability of the algorithm to achieve the goal. All three propulsion schemes were tested and the goal-seeking algorithm was tested alone by moving it in precise, prescribed motions.

4.1 Propulsion

4.1.1   Propulsion Results

The first vessel, designed for complete autonomy was tested in the test pool. While the fins actuated as desired, according to the orientation of the vessel and location of the ultrasonic source, the vessel did not move through the water. Figure 4.1 shows the first vessel in the water.
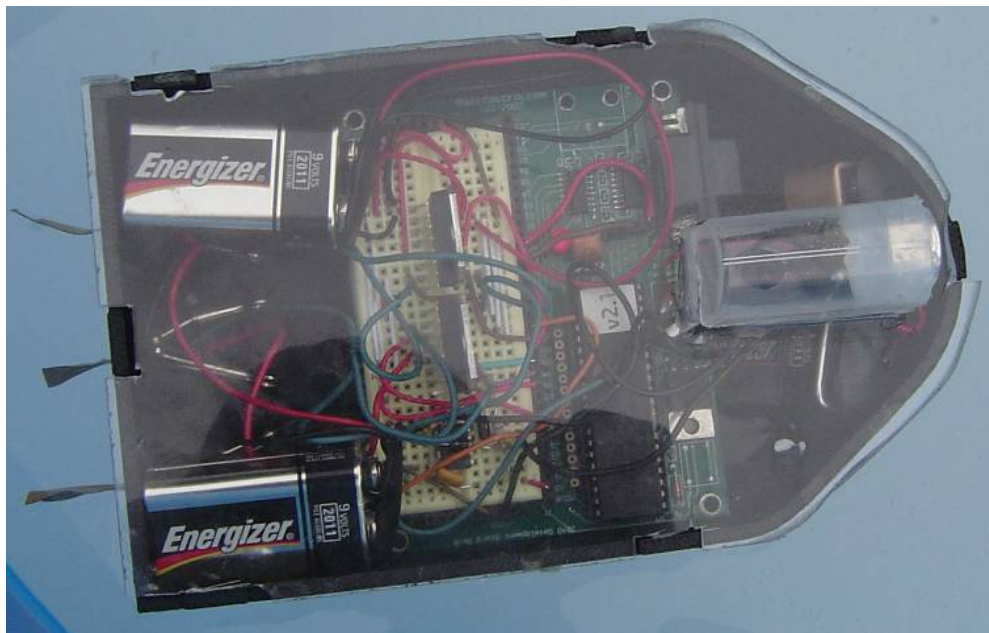
Fig. 4.1: First vessel in test pool with left fin actuating to implement right turn

The second vessel, designed to be light weight, by removing all of the electronic components save for the ultrasonic receiver and electrodes also did not move in the water. In light of this, the fins designed for the IPMC strips were attached and the vessel was tested in the water, and while all strips actuated properly, no results of the propulsion were observed. In spite of the impotent actuation by the IPMC fins, a number of observations were made regarding their actuation:

- Even when every IPMC strip was provided the same PWM duty cycle and same excitation frequency, there was slight variation between strip actuation.

- Independent of delay time between the "high" and "low" signals to the IPMC material, significant quivering was observed during the actuation of just the IPMC strips alone, which was not seen with the addition of the fins.

- Ripples in the water were created during the actuation, showing promise for successful movement.

- With the addition of the fins, to achieve the same angular deflection at the tip, there was a significant decrease in driving frequency.

4.1.2 Propulsion Discussion

The reason for the multiple iterations on the vessel design was to obtain results that yielded propulsion given the amount of actuator material that was available. Where one vessel failed, specific changes were made to address the suspected cause of failure until it could be concluded that there were some significant limitations that could not be

alleviated to yield an autonomous goal-seeking vessel or even an umbilical-dependent vessel.

The first problem seen was during the fitting of the IPMC strips to the vessel and the fins to the IPMC strips. It was impossible to attach the electrodes to the vessel and secure the IPMC material in place without sacrificing some strip length. Likewise, attaching the plastic fins to the IPMC strips was also impossible without sacrificing some length of fins. While the initial strip length was 2.7 cm, attachment to the vessel sacrificed 0.7 cm of length and fin attachment to the IPMC strips sacrificed 0.9 cm of length, yielding only 1.1 cm of effective actuator. This reduction in fin length means the effective actuator mass is only 40% of the actual actuator mass, or reduced from 0.7-g to an estimated effective mass of 0.29-g. Instead of the initial vessel mass to actuator mass ratio of 71, it was increased to 172 when the effective actuator length was considered. Though this is one metric used to compare propulsion schemes, the second vessel with fins attached still had more effective actuator per unit mass of vessel than the biomimetic tadpole.

A second major consideration is the variation between the IPMC material itself from experiment to experiment. In the case of the tadpole experiment, the polymer base was an unspecified Nafion® polymer 0.15 mm thick. The electrodes plated on the polymer base were platinum. The IPMC material used for the purposes of this research used a base polymer of Nafion® 117, 0.18 mm thick with gold electrodes. Though some research has been done comparing the cations saturated in the base polymer [15], no definitive study could be found comparing different polymer bases or various electrodes.

Perhaps one of the most unexpected observations was the reduction in the oscillation frequency of the actuator material when the fins were attached. The IPMC strips alone were initially tuned to a 50% duty cycle with an oscillation frequency of 0.86-Hz. To achieve the same angular tip deflection of 30°, more time was required to move the actuator with the additional load. To move the actuator in one direction with the fins attached required just less than 2 seconds. Therefore, to move the actuator back and forth took 4 seconds, resulting in a 0.25-Hz oscillation frequency. It is important to note that in initial tests with thicker fins no actuation occurred. This indicates some significant limitations of the IPMC material with regards to increasing the fin size. At some point no actuation will occur at all, and no propulsive force would be generated, regardless of fin size.

Though the aforementioned factors could cumulatively contribute to the lack of propulsion, there was no reason more detrimental to the propulsive efforts of the IPMC material than the oscillation frequency. From the impulse-momentum theorem, derived from Newton's second law, it can be shown that the momentum generated by the fins is inversely proportional to the frequency of oscillation. The derivation to obtain the impulse-momentum theorem from Newton's second law is shown in equation 4.1:

$$
\begin{aligned}
F &= ma \\
F &= m\frac{dv}{dt} \\
F \cdot dt &= m \cdot dv \\
\int_0^t F \cdot dt &= \int_{V_0}^{V_f} m \cdot dv \\
\int_0^t F \cdot dt &= mV_f - mV_0
\end{aligned}
\qquad , \qquad (4.1)
$$

where F is the force imparted, t is the time interval used, m the mass of the vessel and V_f and V_0 are the final and initial velocities, respectively. In this case, the best to evaluate the integral on the left hand side of the equation is by discretizing Rosen's force equation for small deflections and integrating for the entire stroke length. It will be assumed that the rate of angular deflection of the IPMC material is constant and the IPMC strip pivots at the vessel body rather than deflecting along the length. Since the static plastic fins account for much of the length and the fin assembly appeared to move steadily and quickly reverted to the neutral position upon a polarity change, these are valid assumptions.

The force was calculated at 5 ms intervals for a total of 10 total seconds. Three propulsion cases were used in the calculations: the IPMC strips with fins attached, the IPMC strips alone, and the fins operating at the frequency of the IPMC strips alone. To obtain the proportional force value for each step, Rosen's equation was modified from its form in (2.7) to obtain the proportional force value as

$$\frac{F}{c} \propto ab \tag{4.2}$$

Where the left side of the equation represents the proportional force value and a and b represent the fin deflection and fin height, respectively. Since the angular velocity $\dot{\theta}$ was assumed to be constant, it was calculated from the frequency f and total angular deflection α in equation 4.3:

$$\dot{\theta} = \frac{f}{2}\alpha \tag{4.3}$$

From (4.3), the angle θ can be found:

$$\theta = \frac{f}{2}\alpha \cdot \Delta t \tag{4.4}$$

The value θ is how much the fin deflects during each time step at a specified frequency. The linear distance or chord length at the fin tip a between steps is:

$$a = L\sin\left(\frac{f}{2}\alpha \cdot \Delta t\right) \tag{4.5}$$

where L is the total fin length from the vessel wall. Substituting this into equation 4.2 results in:

$$\frac{F}{c} \propto L\sin\left(\frac{f}{2}\alpha \cdot \Delta t\right)b \tag{4.6}$$

This equation was utilized in each of the three cases with the parameters listed in table 4.1.

TABLE 4.1: PROPULSION PARAMETERS FOR EACH EXPERIMENTAL CASE

	α	L	b	f
Tadpole Experiment	30	86	62	0.86
IPMC strips alone	30	20	17	0.86
Fins attached	30	86	62	0.25

The parameters listed in table 4.1 were used in (4.6) and their results summarized in table 4.2.

TABLE 4.2: PROPULSION FACTOR COMPARISION BETWEEN EXPERIMENTS

	Tadpole Experiment	IPMC strips alone	Fins attached
Proportional Force Factor	1030×10^{-9}	65.8×10^{-9}	300×10^{-9}
Proportional Impulse Factor	10300×10^{-9}	658×10^{-9}	3000×10^{-9}

Since the proportional force factor at each step is equal to the previous, the proportional impulse factor was the simple sum of all forces over the 10 second time period analyzed multiplied by the time step of 5 ms. Even strictly following Rosen's equation, the tadpole experiment exhibits a greater force than the two experiments performed on the second vessel. Since the mass and velocity of the tadpole is known, the constant that relates force to the fin size can be found.

Comparing the three values in table 4.2 one can see the impact that oscillation frequency has on the propulsion scheme. The fins were designed to operate at a frequency equal to the frequency of the IPMC strips alone, the reduction in operating frequency even at the highest permissible operating voltage was detrimental to the propulsion. Where the propulsive force factor expected was 1030×10^{-9}, the one obtained with the actual 0.25 Hz operating frequency was 300×10^{-9}, 29.1% of what was expected. While this is still 456% greater force than just the IPMC strips alone, it was still not enough for propulsion considering the necessary increase was estimated as greater than 1000%. Assuming that the fins had worked at the frequency of the IPMC strips alone, and given the vessel a 22 mm/s velocity as exhibited by the tadpole, the velocity expected by the fins operating at the reduced frequency can only be 6.4 mm/s at best, moving its entire length, fins included, of 196 mm in 30.6 seconds. Table 4.3 compares the speed normalized to length of the research vessel to other vessels and fish that move through the water.

TABLE 4.3: COMPARISON OF VARIOUS ANIMALS AND VESSELS SPEED IN WATER RELATIVE TO BODY WEIGHT

Naval species	Length [m]	Typical Travelling Speed [m/s]	Normalized Speed to Length [L/s]
Tadpole [24]	0.05	0.376	8.000
Boxfish [25]	0.12	0.456	3.800
Great white shark [26]	6.00	11.200	1.867
Tadpole experiment	0.10	0.024	0.246
Blue Whale [27]	30.00	5.556	0.185
USS Enterprise Aircraft Carrier [28]	342.30	15.556	0.045
Second vessel with fins	0.20	0.009	0.045

The data in table 4.3 shows is how the IPMC propelled vessel compares to numerous aquatic species, ranging from fish to tadpoles to aircraft carriers. Had the vessel created for the purpose of this research operated with the desired fin frequency, it would have had normalized speeds relative to that of an aircraft carrier. However, at the time of this writing, the USS Enterprise is the longest naval vessel in the world, has 8 nuclear reactors aboard, and weighs nearly 90×10^6 kg. The two species with the most similar propulsion mechanism, lateral dorsal fin oscillation, are the great white shark and the boxfish, and both have normalized sustained speeds two orders of magnitude greater than that of the research vessel with fins. The propulsion of a tadpole is somewhat different as it undergoes undulatory lateral motion at higher frequencies yielding a constant propulsive force effort.

The vessel created for the research is essentially using a fish' means of propulsion contained in a man-made container. The major difference between fish fin propulsion and the IPMC strips on the rear of the research vessels is the lack of motion along the length. Fish can be up to 80% muscle, most of which is along the length of the fish body [29]. In contrast, the useable IPMC material only accounts for 0.58% of the vessel weight. A fish curves its entire body as it swims which is one difference between the vessel and fish motion. On the other hand, the IPMC strips only flex at the rear and do not have any effect on the orientation of the vessel itself. In all modern self-propelled boats, the propulsion scheme yields a constant force. Conversely, the IPMC strips provide only intermittent propulsive force, as there is some time for acceleration and deceleration of the fins at the end of their stroke including some delay to return to the neutral position.

While Rosen's equation is very useful for determining fin propulsion, it does not account for various fin shapes and the fluid mechanics involved in the propulsion. First of all, the only two fin parameters in Rosen's equation are the amplitude of oscillation and the height of the fin. The amplitude of oscillation is simply a function of the fin length and its angular deflection. Therefore, Rosen's equation only considers the overall size of the fin, or the size rectangle the fin would fit in. Of course this was considered when constructing the fins, by cutting them in a triangular shape to maintain surface area and decrease the mass. If a T-shaped fin instead of a triangular fin where the height and length were both the same size, it would not be a difficult to see how the triangular fin could generate more propulsive force than the T-shaped fin.

The umbilical wire could have had some negative impact on the propulsion of the vessel. However, it was accounted for during testing as it was held up and positioned so it would have as little impact on the vessel's motion as possible in that specific orientation. Nevertheless, had the vessel moved, the umbilical wire would likely have held it back as any propulsive efforts would have been unable to overcome the weight and forces imparted by the umbilical wire.

4.2 Goal-seeking Algorithm

4.2.1   Goal-seeking Results

Regardless of the poor actuation of the IPMC material, the goal-seeking algorithm was tested and recorded on land. The C code was rewritten and all PWM portions were replaced with a line of text indicating what action should be performed (right, left, or forward) and a prompt that allowed the user to wait for a button press after the boat had been moved (located in Appendix B.2). Since the actuators were not sufficient to move the boat, it was manually moved according to the goal-seeking algorithm. Upon receipt of a turning command, the sensor apparatus was rotated 20° in the proper direction. When a forward command was received, the apparatus was moved approximately 30 to 35 cm in the direction which the apparatus faced. A tape measure was laid down along the transmitter axis and markers were placed every 30 cm as a reference.

The first test of the algorithm began 240 cm away from the ultrasonic transmitter and 30 cm to the left of the transmitter axis. Upon collision with the transmitter, the vessel was just stopped as close as possible. Figure 4.2 shows the first test.

Fig. 4.2: First test of goal-seeking algorithm, 240 cm away, 30 cm off-center, 8 total iterations

The second test of the goal-seeking algorithm began 120 cm away from the transmitter and 60 cm to the left of the transmitter axis. Figure 4.3 shows the second trial.

Fig. 4.3: Second test of goal-seeking algorithm, 120 cm away, 60 cm off-center to the left, 6 total iterations

The third test was set up as a mirror image of the second test, 120cm away from the transmitter and 60 cm to the right. Figure 4.4 shows this test.

Fig. 4.4: Third test of goal-seeking algorithm, 120 cm away, 60 cm off-center to the right, 6 total iterations

The results of the three tests performed are summarized in Table 4.4 and show the final operation at each sampling step (position) and the order in which each command was implemented.

TABLE 4.4: STEPS TO ACHEIVE GOAL FOR EACH TRIAL

Step	Trial 1 (front)	Trial 2 (left)	Trial 3 (right)
1	Right	Left	Right
2	Straight	Right	Straight
3	Left	Left	Right
4	Right	Left	Left
5	Left	Straight	Right
6	Right	N/A	N/A
7	Left	N/A	N/A

These three tests show that the goal-seeking algorithm successfully reaches the goal each time when placed in front of it. This analysis did not include the circumstance when the receiver is placed behind the transmitter or out of its range. The way the algorithm is set up, the receiving apparatus will not move towards the transmitter, but only move around in circles until it gets some input on channel A0. However, since this was not the case in any of the three tests, the apparatus successfully moved to the goal.

One test of the efficiency of this code can be done by examining the distance from the goal and the number of steps in the sequence. Table 4.5 shows the comparison between distance from goal and steps to achieve it.

TABLE 4.5: COMPARISON OF ALGORITHM TRIALS

Test	Distance away (cm)	Iterations
Goal to the front (1)	241.9	7
Goal to the left (2)	134.2	5
Goal to the right (3)	134.2	5

This comparison gives an average distance per iteration of 34.6 cm when the goal is to the front and 26.8 cm when the goal is off to the side. The most likely reason for this difference is because the final iteration when the goal off to the side was not the full 30 cm, but rather something closer to 10 cm because the apparatus had achieved the goal. Removing this fifth iteration gives an average distance per iteration of 33.6 cm, much closer to the results from the straight-on approach.

4.2.2 Goal-seeking Discussion

These three tests show that the goal-seeking algorithm is very efficient in traveling towards the goal. The first test shows that the apparatus moves towards the axis sooner than it moves closer to the goal (Figure 4.2). This is because it is at the transmitter axis where the ultrasonic signal is the strongest, even when the apparatus is somewhat closer to the transmitter but off the axis (Figures 4.3 and 4.4). The second and third tests show how effective the turning towards the goal is. Though the signal is not near as strong off-axis as it is on the axis, there is still some reception. The apparatus turns towards the axis three times in each of the second two tests. In the test to the right

of the receiver axis, the apparatus turned away from the axis once. Despite this "mistake" or probable erroneous reading of the ultrasonic transmission, the apparatus still reached the goal in only six iterations.

While implementing the goal-seeking algorithm to test its ability to guide a vessel towards a goal, a few observations were made regarding the ultrasonic signal utilized. First of all, the amplitude of the signal picked up just at the 3-m mark was extremely low meaning without extensive signal processing, the amplitude of the ultrasonic signal could not be determined with confidence at this distance. Secondly, the threshold (set to 250, only 6 divisions below the maximum value that could be obtained) was not reached until the vessel was within 10 cm of the ultrasonic source, showing the range was from 10 cm to 3-m. Finally, there was no significant difference between the amplitudes obtained in the second and third trials, meaning there was virtually no difference in signal strength on either side of the emitter axis.

The implementation of the goal-seeking algorithm also gave some insight into how it would operate in various conditions. The first actuation instruction given is to make a right turn by actuating the left fin. If the signal obtained here is greater, the algorithm tells the vessel to travel in that direction. Given two circumstances in which the vessel is equidistant to the goal in both, but one requires more left turns than right turns, the one requiring more right turns will travel toward the goal faster than the one requiring more left turns. This is because if the signal amplitude measured after the right turn is less than the signal measured in the first position the vessel will turn left twice and compare the first position to the leftmost position, taking significantly longer time

because there are two more actuations required before going forward. If the strongest

signal is measured at the first position, the vessel travels toward the target slower still

because an additional fin actuation would be required on top of what it takes to travel

toward the leftmost position. Table 4.6 shows the number of turn instructions for each

step.

TABLE 4.6: FIN ACTUATIONS TO DIRECT VESSEL IN A CERTAIN DIRECTION

Direction of travel	Number of actuations required
Right	1
Left	3
Straight	4

Using the above table, one can estimate the time to target. The time to acquire

the amplitude of the ultrasonic signal via port A0 is negligible, so the sum of the turning

fin strokes can be added arithmetically. To travel forward 30 cm in the best conditions

takes approximately 12 se at 25 mm/s, the top speed of any IPMC propelled vessel in

any prior research. The assumption is made that to implement a left or right turn by

actuation the right or left fin, respectively, takes 5 s. By this assumption, and Table 4.3,

to turn right takes 5 s, turning left takes 15 s, and continuing forward takes 20 s. How to

add this information together to generate an estimated time to target is shown in (4.7).

$$\text{Time to target} = 5R + 15L + 20F + 12i , \qquad\qquad (4.7)$$

where R is the number of right turns, L is the number of left turns, F is the

number of times the vessel continued in its prior trajectory, and i is the number of

iterations performed.

Using the aforementioned equation, an estimate of time to target for each of the three trials was produced in conjunction with Table 4.1. For instance, to determine the time to target for the first trial, there were a total of seven iterations, three right turns and three left turns and one forward motion. Substituting these numbers into (4.8) gives:

$$
\begin{aligned}
\text{Time to target} &= (5 \times 3) + (15 \times 3) + (20 \times 1) + (12 \times 7) \\
\text{Time to target} &= 15 + 45 + 20 + 84 \\
\text{Time to target} &= 164
\end{aligned}
\tag{4.8}
$$

Therefore the time to target for the first trial, at 240 cm away from and 30 cm to the side of the transmitter axis was 164 s, giving an average speed of 14.8 mm/s. The time to target for each of the three trials and their average speeds is shown in Table 4.7.

TABLE 4.7: ESTIMATE OF TIME TO TARGET AND AVERAGE SPEED FOR EACH GOAL-SEEKING TRIAL

Trial	Time to Target (s)	Average Speed (mm×s^{-1})
1	164	14.8
2	130	10.3
3	110	12.2

Table 4.7 shows that under the assumptions stated for turning time and traveling speed, there is really only a little statistical difference between the average speeds. However, the best comparison that could be made was between trials two and three, which were symmetric about the transmitter axis. These two trials were completely opposite from each other when it came to the commands given by the goal-seeking algorithm. Trial two had three left turns and one right turn over five iterations where trial three had three right turns and one left turn over five iterations. There is an 18.2% increase in the time to target from trial three to trial two, only due to the addition of the left turns.

One additional observation made regarding the goal-seeking algorithm was how the apparatus would move in the absence of any signal. Due to the nature of the "if" statement in C, when stated as "if(x>y)" where both x and y are equivalent, no comparison is made so the instruction is ignored and the code would continue as if nothing had been there. This was the case with the goal-seeking algorithm where it compared $V0$, the initial signal in the front direction, and $V1$, the signal obtained after turning right. When both are equivalent, the algorithm will skip to the end of the C code where the vessel is instructed to go forward and read another signal. This is done after the vessel has turned right. Therefore, when there is no ultrasonic signal present, the algorithm will send the instruction to go right then move forward each time, eventually traveling in a full circle.

4.2.3   Goal-Seeking Algorithm Improvements

To enhance the effectiveness and time to target of the current goal-seeking code, a number of improvements and adjustments could be made. First, the code could be modified so that the vessel turns away from a poor signal sooner and only travels towards the greatest signal instead of the greatest signal obtained in three directions. This would permit the vessel to start at virtually any position and search for the strongest signal in any direction.

After taking the first ultrasonic amplitude reading, one left fin stroke could be implemented and then another reading could be taken. If this second measured value is less than the first reading, the vessel would turn back towards the left by implementing a right fin stroke. A reading would be taken and compared to the previous reading. If this value is greater, the vessel would continue to turn and read as until it encounters a lesser value, turn back in the opposite direction and then travel forward some distance. If the second measured value is greater than the first value obtained, the vessel should continue rotating right until it reads a smaller value, turns back left once and travels forward. Figure 4.5 shows a flow chart of how this new code might be implemented.
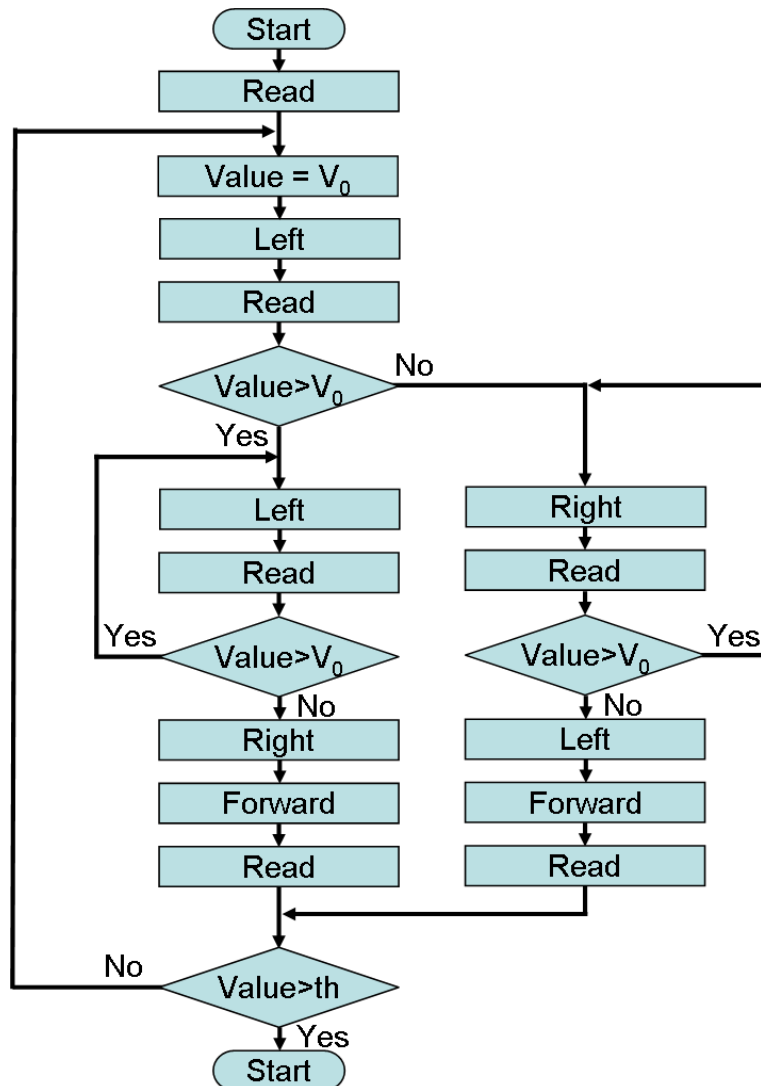
Fig. 4.5: Flow chart for proposed goal-seeking algorithm

As with the implemented goal-seeking algorithm, there is a problem with the directionality of the ultrasonic source. If an ultrasonic signal is still desired, the best means to implement it would be to ensure a planar source instead of the linear source used for the experiments. Multiple transmitters could be placed about a circular perimeter at certain intervals to ensure the ultrasonic signal could be "seen" from all approaches. Figure 4.6 depicts the proposed scheme. With this new transmission

scheme, any vessel starting position or orientation should be viable as long as the vessel

stays within range of the ultrasonic transmitters.
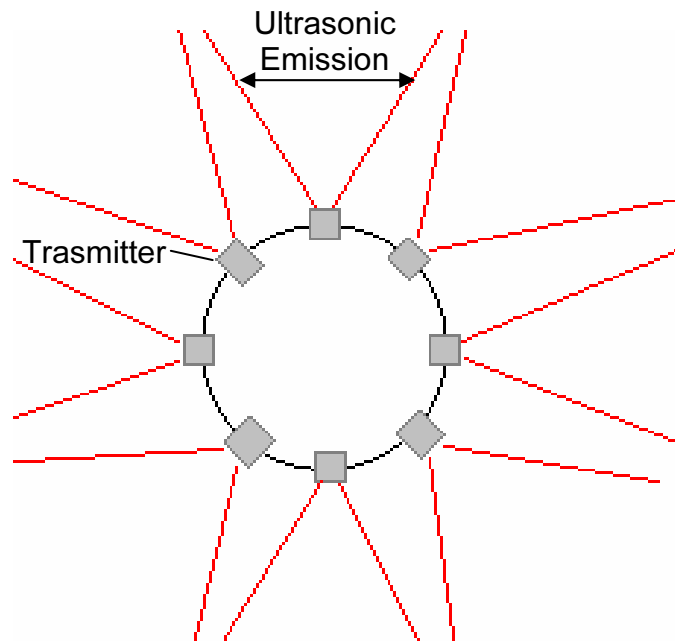
Fig. 4.6: New ultrasonic transmission scheme

In summary, the new goal seeking algorithm will have a faster time to target

because it does not double back on itself to arrive at a previous orientation. It simply

seeks the highest amplitude signal in a direction, continues to search for a higher

amplitude signal in that same direction and travels towards it. Using a more

comprehensive source to generate ultrasonic signals in all directions would allow for the

algorithm to be used in virtually any setting, as long as the vessel is within the range of

the transmitters.

5   CONCLUSIONS

The procedure described in this thesis to create an autonomous vehicle propelled by IPMC fins was unsuccessful. Significant lightening and even redesign of the vessel by using an umbilical cord to transmit power and the ultrasonic signal to and from the microcontroller was done in an attempt to produce a self-propelled vessel. Both vessels were unable to move in the water despite optimal actuation by the IPMC strips alone and even the IMPC strips with the fins added.

Prior research has been done with various sized vessels and various IPMC strip sizes. The most notable difference between the two vessels created for the purpose of this research and the prior creations was fin size and overall vessel mass. The vessels created were more massive and had a smaller fin than any prior creations. This led to the addition of fins sized according to an equation proposed by Rosen [23] called the vortex peg hypothesis.

To use this IPMC material in any real world environment is unfeasible at this time. The IPMC material used as a fin may have generated some propulsive force, but the low mass of the second test vessel was easily moved by external forces such as the slightest wind gust or motion in the test pool. Even the reaction forces due to the umbilical wires proved to be too much for stable boat operation.

A number of rationalizations were considered to explain the inability of the IMPC strips, even with properly sized fins attached to propel the vessel forward. Perhaps the most detrimental reason was the reduced frequency of the actuators with the IPMC strips attached. The observed frequency to obtain the desired 30° deflection in

either direction was 29% of the 0.86 Hz seen with the IPMC strips alone. Another short-coming was the variation of the IPMC material itself. The IPMC material shows some variation even when two strips are cut from the same sheet. Furthermore, different IPMC variations exist. The composite used for this research was Nafion® 117 with gold plating, but the composite in the tadpole experiment was an unknown Nafion® polymer with platinum plating. It was determined that these three factors, along with a number of other less significant factors largely contributed to the inability of the IPMC actuator to propel the vessel.

Through the literature survey, the IPMC material has been used in a number of biomimetic applications. The three robots studied, the ray [12], tadpole [13], and snake [15] all used undulatory or wave-like motion either in a single IPMC strip as with the tadpole or the sum result of multiple strips as with the ray and snake. In the case of the tadpole and ray, this results in a constant propulsive effort as the fin or propulsive surface is always moving to propel the vessel forward. In the case of the biomimetic fins created for the purposes of this research there is a deceleration and acceleration of the fins as they reach the limits of their stroke.

From the observations made regarding the ultrasonic signal, it can be concluded that in the form presented in this experiment, ultrasonic signals obtained by transducers are too weak to be used in long-range applications. However, they are very accurate over short distances, giving predictable and reproducible results every time. Ultrasonic signals are highly directional and it does not take much deviation from the transmitter axis to significantly reduce the signal amplitude.

The goal seeking algorithm's ability to travel towards a goal with only one signal receiver was demonstrated. By essentially using the one receiver as three by turning the vessel, simple comparisons can be made to give the next instruction. This allows for very little additional vessel weight from sensors. However, the addition of a second or third sensor would require the additional circuitry to process the signal so it could be read independently from the other sensors. Because this processing requires an op-amp to both amplify and rectify the signal, this would require more on-board power or less operating life.

From the research performed and prior research studied, some conclusions can be made:

- As a fin propelling a significantly large-sized vessel, IPMC material is ineffective as it cannot generate the propulsive force required to move the vessel through the water.

- To generate significant propulsive force, a large amount of fin surface area is required, which reduces the oscillation frequency of the IPMC strips.

- Using IPMC material as a fin in a real-life environment with wind and waves is impractical because any external forces imparted would easily blow a light-weight vessel off course, negating the propulsive effects of the fins.

- Control of a specific fin's bending motion is unnecessary if it only needs to oscillate. The average PWM voltage must be tuned to allow for the best actuation while the frequency of oscillation must be tuned to allow for the least relaxation and full actuation in both directions.

- While a goal-seeking algorithm using only one sensor is efficient in that it consumes less power and weighs less than using multiple sensors, it requires more steps to find the direction to the target, increasing both processing time and time to target.

- In the specific goal-seeking algorithm used, time to target was increased when the number of left turns was increased because this required three turn commands rather than only one.

- Use of an ultrasonic scheme to direct an autonomous vehicle is practical only over short distances unless very clean, noiseless devices are used to filter the specific frequency and amplify and process it for data acquisition purposes.

- Using a microcontroller in a goal-seeking application is quite feasible. All power amplification devices such as H-bridges or Darlington pairs can be used in conjunction with the microcontroller on a development board and the analog port allows for data acquisition.

As an actuator, the IPMC material works. However, this research has shown that there should be some significant reservations about using this material as an actuator on a large scale in the "real world." Even in laboratory tests, the material generates only a miniscule force when used as a propulsor, resulting in impractical velocities for applications outside of the laboratory.

To implement a goal seeking algorithm using only one sensor proved difficult and did have its drawbacks regarding performance. With some tuning and further

experimentation, however, this scheme of control on a larger scale is very effective with

respect to weight and sensor power consumption.

REFERENCES

[1]   Unknown Author, "Water Clock" [Online document], cited Sep. 13, 2006.

        Available: http://en.wikipedia.org/wiki/Water_clock.

[2]   Unknown Author, "Nikola Tesla" [Online document], cited 2006 Sep. 13, 2006.

        Available: http://en.wikipedia.org/wiki/Nikola_Tesla.

[3]   Unknown Author, "Shakey the Robot" [Online document], cited Sep. 13, 2006.

        Available: http://en.wikipedia.org/wiki/Shakey_The_Robot.

[4]   Unknown Author, "History of Artificial Intelligence" [Online document], cited

        Sep. 13, 2006. Available:

        http://en.wikipedia.org/wiki/History_of_Artificial_Intelligence.

[5]   Unknown Author, "Darpa Grand Challenge" [Online document], cited Sep. 13,

        2006. Available: http://en.wikipedia.org/wiki/Darpa_grand_challenge.

[6]   Unknown Author, "Electroactive Polymers" [Online document], cited Sep. 13,

        2006. Available: http://en.wikipedia.org/wiki/Electroactive_polymers.

[7]   Y. Bar-Cohen, S. Leary, A. Yavrouian, K. Oguro, S. Tadokoro, J. Harrison, J.

        Smith and J. Su, "Challenges to the Application of IPMC as Actuators of

        Planetary Mechanisms," in *Proceedings of the SPIE's Annual International

        Symposium on Smart Structures and Materials*, March 2000, pp. 1 – 6.

[8]   K. J. Kim and M. Shahinpoor. "Ionic Polymer-Metal Composites: IV. Industrial

        and Medical Applications." *Smart Materials and Structures*, vol. 14, pp. 197–

        214, 2005.

[9]   K. Yun and W.-J. Kim, "Microscale Position Control of an Electroactive Polymer Using an Anti-Windup Scheme," *Smart Materials and Structures,* vol. 15, pp. 924-930, 2006.

[10]   Y. Bar-Cohen, M. Shahinpoor, J. O. Simpson, and J. Smith, *Ionic Polymer-Metal Composites (IPMC) As Biomimetic Sensors, Actuators, & Artificial Muscles – A Review.* Albuquerque, NM: University of New Mexico, 2004.

[11]   H. C. Park, K. J. Kim, S. Lee, S. Y. Lee, Y. J. Cha, N. S. Goo, and K. J. Yoon, "Biomimetic Flapping Devices Powered by Artificial Muscle Actuators," UKC2004 US-Korea Conference on Science, Technology and Entrepreneurship, August 2004.

[12]   A. Aabloo, M. Anton, M. Kruusmaa, and A. Punning, "A Biologically Inspired Ray-like Underwater Robot with Electroactive Polymer Pectoral Fins," in *Proceedings of the International IEEE Conf. Mechatronics and Robotics 2004 (MechRob'04)*, 2004, vol. 2, pp. 241–245.

[13]   J. Jung, B. Kim, J.-O. Park, and Y. Tak, "Undulatory Tadpole Robot (TadRob) Using Ionic Polymer Metal Composite (IPMC) Actuator," in *Proceedings of the 2003 IEEE/RSJ Intl. Conference on Intelligent Robots and Systems*, Oct. 2003, pp. 2134–2138.

[14]   K. J. Kim, J. W. Paquette, and W. Yim, "Aquatic Robotic Propulsor Using Ionic Polymer-Metal Composite Artificial Muscle," in *Proceedings of the 2004 IEEE/RSJ International Conference on Intelligent Robots and Systems*, Sep. 2004, pp. 1269–1274.

[15]   K. Asaka, N. Kamamichi, T. Kozuki, Z.-W. Luo, and M. Yamakita, "A Snake-Like Swimming Robot Using IPMC Actuator and Verification of Doping Effect," in *Proceedings of the 2005 IEEE/RSJ International Conference on Intelligent Robots and Systems*, Aug. 2005, pp. 2035–2040.

[16]   EAMEX Corporation. Ion Conductive Actuator. [Online], cited Aug. 3, 2006. Available: http://www.eamex.co.jp/ion_e.html#bio.

[17]   B. Belkhouche, F. Belkhouche, and P. Rastgoufard, "Line of Sight Robot Navigation Toward a Moving Goal," *IEEE Trans. on Systems, Man, and Cybernetics – Part B: Cybernetics*, vol. 36, no. 2, pp. 255–267, Apr. 2006.

[18]   H.-L. Huang, C.-H. Kuo, and M.-Y. Lee, "Development of Agent-Based Autonomous Robotic Wheelchair Control Systems," *Biomedical Engineering – Applications, Basis & Communications*, vol. 15, no. 6, pp. 223–234, Dec. 2003.

[19]   V. Callaghan, M. Colley, and H. Hagras, "Outdoor Mobile Robot Learning and Adaptation," *IEEE Robotics and Automation Magazine*, vol. 8, no. 3, pp. 53–69, Sep. 2001.

[20]   J. Bay, "Design of the 'Army-Ant' Cooperative Lifting Robot," *IEEE Robotics and Automation Magazine*, vol. 2, no.1, pp. 36–43, Mar. 1995.

[21]   J. Borenstein and I. Ulrich, "The GuideCane – A Computerized Travel Aid for the Active Guidance of Blind Pedestrians," in *Proceedings of the IEEE International Conference on Robotics and Automation*, Apr. 1997, pp. 1283–1288.

[22]   Microchip Technology Inc. Home Page. [Online], cited Sep. 13, 2006.

Available: http://www.microchip.com

[23]   M.W. Rosen, *Water Flow about a Swimming Fish*. China Lake, CA: U.S. Naval

Ordnance Test Station TP 2298, 1959.

[24]   H. Liu, R. Wassersug, and K. Kawachi, "A Computational Fluid Dynamic Study

of Tadpole Swimming," *Journal of Experimental Biology*, vol. 199, pp. 1245–

1260, Feb 29, 1996.

[25]   J.R. Hove, L.M. O'Bryan, M.S. Gordon, P.W. Webb, and D. Weihs, "Boxfishes

(Teleostei: Ostraciidae) as a Model System for Fishes Swimming with Many

Fins: Kinematics," *Journal of Experimental Biology*, vol. 204, pp. 1459–1471,

Jan. 30, 2001.

[26]   Unknown Author, "Great White Shark" [Online document], cited Nov. 15, 2006.

Available: http://en.wikipedia.org/wiki/Great_White_Shark.

[27]   Unknown Author, "Blue Whale" [Online document], cited Nov. 15, 2006.

Available: http://en.wikipedia.org/wiki/Blue_Whale.

[28]   Unknown Author, "USS Enterpise (CVN-65)" [Online document], cited Nov. 15,

2006. Available: http://en.wikipedia.org/wiki/USS_Enterprise_(CVN-65).

[29]   P. Pitts, "How Fish Swim" [Online document], cited Nov. 16, 2006. Available:

http://mdc.mo.gov/kids/out-in/2001/02/2.htm.

Supplemental Sources Consulted During Research

D. Alciatore and M. Histand, *Introduction to Mechatronics and Measurement Systems*,
2nd ed. Boston, MA: McGraw Hill, 2003.

T. Beckwith, J. Lienhard V, and R. Marangoni, *Mechanical Measurments*, 5th ed.
Reading, MA: Addison-Wesley, 1993.

A. Budak, *Passive and Active Network Analysis and Synthesis*. Boston, MA: Houghton
Mifflin , 1974.

A. Emani-Naeini, G. Franklin, J. Powell, *Feedback Control of Dynamic System*s, 4th ed.
Upper Saddle River, NJ: Prentice Hall, 2002.

J Millman J. Microelectronics: *Digital and Analog Circuits and Systems*. New York:
McGraw-Hill, 1979.
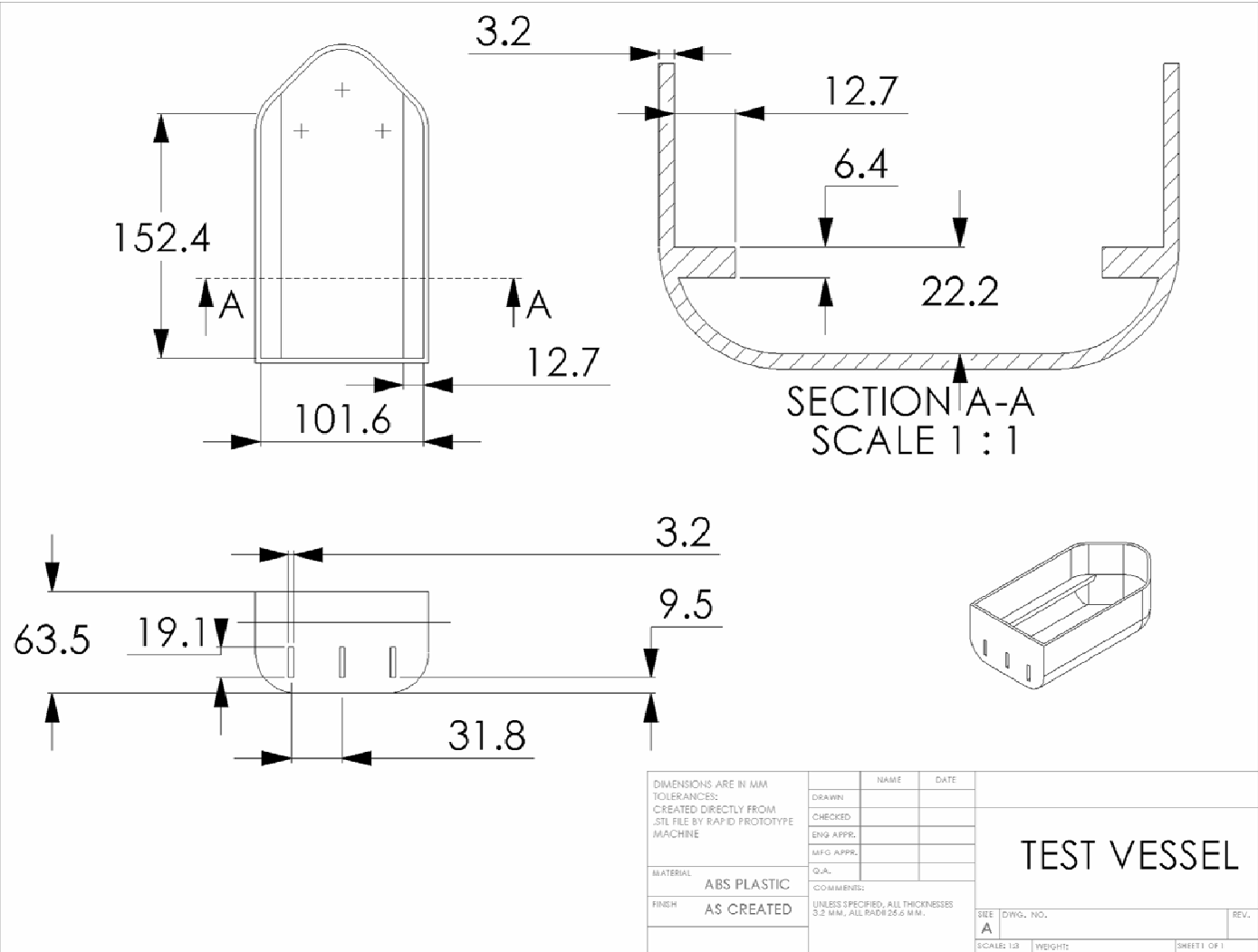
Fig. A.1: Dimensioned drawing for first test vessel

APPENDIX B

B.1 First Goal-Seeking Code

```
#include <16F877.h>

#use delay(clock=10000000)

#use rs232(baud=9600, xmit=PIN_C6, rcv=PIN_C7)


//Pin designations:

//B0 = right fin, right electrode

//B1 = open

//B2 = open

//B3 = right fin, left electrode

//B4 = middle fin, right electrode

//B5 = middle fin, left electrode

//B6 = left fin, right electrode

//B7 = left fin, left electrode


int stroketime;

int strokecount;

int i;

int j;

long th;

long v1;
```

```
long v0;

long value;


//Move Forward

forward()

{

        for (strokecount=0;strokecount<15;strokecount++)

        {

                for (i=0;i<stroketime;i++)

                {

                        output_b(0x51);

                        delay_ms(20);

                        output_b(0x00);

                        delay_ms(20);

                }

                output_b(0x00);

                delay_ms(200);

                for(i=0;i<stroketime;i++)

                {

                        output_b(0xa8);

                        delay_ms(20);

                        output_b(0x00);
```

```
                    delay_ms(20);

            }

            output_b(0x00);

            delay_ms(400);

        }

}


//Turn Right

right()

{

        for (strokecount=0;strokecount<10;strokecount++)

        {

                for (i=0;i<stroketime;i++)

                {

                        output_b(0x40);

                        delay_ms(20);

                        output_b(0x00);

                        delay_ms(20);

                }

                output_b(0x00);

                delay_ms(200);

                for(i=0;i<stroketime;i++)
```

```
                    {
                            output_b(0x80);

                            delay_ms(20);

                            output_b(0x00);

                            delay_ms(20);

                    }
                    output_b(0x00);

                    delay_ms(400);

            }

    }


//Turn Left

left()

{

        for(strokecount=0;strokecount<10;strokecount++)

        {

                for (i=0;i<stroketime;i++)

                {

                        output_b(0x08);

                        delay_ms(20);

                        output_b(0x00);

                        delay_ms(20);
```

```
                }

                output_b(0x00);

                delay_ms(200);

                for(i=0;i<stroketime;i++)

                {

                        output_b(0x01);

                        delay_ms(20);

                        output_b(0x00);

                        delay_ms(20);

                }

                output_b(0x00);

                delay_ms(400);

        }

}


//Read Ultrasonic Signal

read()

{

        value = read_adc();

}


//main code
```

```
main()

{

setup_adc_ports(RA0_ANALOG);

setup_adc(ADC_CLOCK_INTERNAL);

set_adc_channel(0);

value = 0;

stroketime = 7;

th = 225;

        while(value<=th)

        {

        //sample three values

        read();

        v0 = value;

        printf("v0 is %lu\n\r",v0);

        right();

        read();

        v1 = value;

        printf("v1 is %lu\n\r",v1);

        if(v0>v1)

                {

                left();

                left();
```

```
        read();

        v1 = value;

        printf("v1 is now %lu\n\r",v1);

        }

    if(v0>v1)

        right();

    forward();

    read();

    }

}
```

B.2 Amended Goal-Seeking Code for Manual Control

```
#include <16F877.h>

#use delay(clock=10000000)

#use rs232(baud=9600, xmit=PIN_C6, rcv=PIN_C7)


long th;

long v1;

long v0;

long value;


//Move Forward

forward()

{

printf("Move boat forward\n\r");

printf("Press any key when done\n\r");

getc();

}


//Turn Right

right()

{

printf("Move boat right\n\r");
```

```
printf("Press any key when done\n\r");

getc();

}


//Turn Left

left()

{

printf("Move boat left\n\r");

printf("Press any key when done\n\r");

getc();

}


//Read Ultrasonic Signal

read()

{

        value = read_adc();

}


//main code

main()

{

setup_adc_ports(RA0_ANALOG);
```

```
setup_adc(ADC_CLOCK_INTERNAL);

set_adc_channel(0);

value = 0;

th = 245;

        while(value<=th)

        {

        //sample three values

        read();

        v0 = value;

        printf("v0 is %lu\n\r",v0);

        right();

        read();

        v1 = value;

        printf("v1 is %lu\n\r",v1);

        if(v0>v1)

                {

                left();

                left();

                read();

                v1 = value;

                printf("v1 is now %lu\n\r",v1);

                }
```

```
if(v0>v1)

        right();

forward();

read();

}

}
```

APPENDIX C

```matlab
clc

clear all

close all


t = 0:1/4000:1/10;

x = 0.100*sin(40*2*pi*t);


figure(1)

plot(t,x)

xlabel('Time (ms)')

ylabel('Signal amplitude (V)')

grid on


figure(2)

for i=1:1:length(x)

    if x(i)<=0

        y(i)=0;

    else

        y(i)=x(i);

    end

end
```

```matlab
plot(t,y,'r')

xlabel('Time (ms)')

ylabel('Signal amplitude (V)')

grid on


figure(3)

plot(t,y*50)

xlabel('Time (ms)')

ylabel('Signal amplitude (V)')

grid on


s = tf('s')

filter = 1/(1/20*s+1);


figure(4)

lsim(filter,y*50,t);

xlabel('Time (ms)')

ylabel('Signal amplitude (V)')
```

VITA

Jason Aaron Vickers was born in Anchorage, Alaska in the winter of 1982. Most of his life was spent overseas in Indonesia and Ecuador before he returned to the United States to attend Texas A&M University in College Station, TX. Completing his degree of Bachelor of Science in mechanical engineering in only 3 ½ years, he made the decision to continue pursuing his studies at Texas A&M and enrolled in the Masters of Science program.

He currently works for Mustang Engineering in Houston, Texas in the Automation and Control Department and aspires to one day work in the aerospace or defense industries.

His permanent address is:

402 Waterside Dr.
Lafayette, LA 70503
(337) 981-4206

His current address is:

2919 Fresco Dr.
Katy, TX 77449
(281) 567-9790

His e-mail address is:

javick82@gmail.com